UNIVERSITY OF NAPLES FEDERICO II

DEPARTMENT OF VETERINARY MEDICINE AND ANIMAL PRODUCTIONS

Ph.D. program in Biology, Pathology and Environmental Hygiene in Veterinary Medicine (Cycle XXVIII)

Coordinator: Prof. Giuseppe Cringoli

TITLE

Lysosomal protease cathepsin D, new driver of apoptosis during acute kidney injury

Driving lecturer:
Prof. Luigi Avallone

Candidate:
Dr. Pasquale Cocchiaro

Tutor:
Prof. Luigi Michele Pavone

Co-tutor:
Dr. Anna Moles

2015/2016

ACKNOWLEDGEMENTS

Firstly, I would like to thank my supervisor, Professor Luigi Michele Pavone for giving me the opportunity to pursue a PhD, for his patience, motivation, enthusiasm, and immense knowledge. I would like to express my sincere gratitude to my other supervisor Dr Anna Moles for her continuous support throughout my research and for her guidance. She has always helped me with my research and also with my thesis. I could not have imagined having a better supervisor and mentor for my PhD I would like to thank Professor Derek Mann for giving me the opportunity to spend the last years of my PhD at Newcastle University in the Fibrosis group. Professor Neil Sheerin for his advice and support during this thesis. Professor Paola Di Natale and Professor Emmanuele De Vendittis for their valuable advice, Professor Luigi Avallone, Professor Norma Staiano, Dr Fiona Oakley, Dr Jelena Mann for their contribution to this PhD.

I want to express my gratitude to Giuliana Cerulo, Patrizia Sarogni, Valentina Villano and Ciro Ruggiero for the stimulating discussions, for the work and for all the fun time spent in the lab together. My thank goes to all the members of the Fibrosis Group, for their strong patience and support. They helped me every day and for all the good time spent in the lab. Particularly, I would like to acknowledge Dr. Luigi Locatelli, Christopher Fox, Samir Luli, Dr Pier Paioli and Dr Eva Moran for the many valuable discussions that helped me to understand my research better.

I would like to thank all my friends and all the people that I have met during this experience, they have all contributed to my personal and professional development.

My biggest love and an utmost thank goes to my family and Maria. The presence of them in my life is more important than any achievement.

INDEX

1. INTRODUCTION

1.1.1. Kidney anatomy and physiology

The kidneys are organs that serve several essential regulatory roles in vertebrate animals. They are reddish-brown, bean-shaped organs located in the abdominal cavity, more specifically in the paravertebral gutter, and lie in a retroperitoneal position at a slightly oblique angle. There are two kidneys, one on each side of the spine. The asymmetry within the abdominal cavity caused by the liver typically results in the right kidney being slightly lower than the left, and left kidney being located slightly more medial than the right. The left kidney is typically slightly larger than the right kidney [1] (Fig. 1). The superior pole of the right kidney is adjacent to the liver. For the left kidney, it is next to the spleen. Both, therefore, move down upon inhalation. In humans, the upper pole of each kidney lies opposite the twelfth thoracic vertebra, and the lower pole lies opposite the third lumbar vertebra. The weight of each kidney ranges from 125 g to 170 g in men and from 115 g to 155 g in women. The human kidney is approximately 11 cm to 12 cm in length, 5.0 cm to 7.5 cm in width, and 2.5 cm to 3.0 cm in thickness.

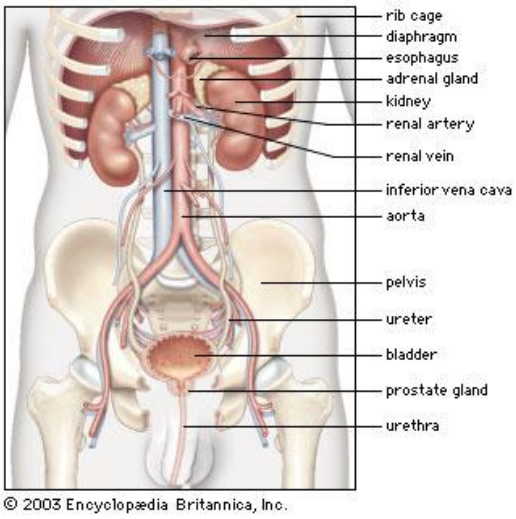

Figure1: Location of the kidneys in the human body. Extracted from http://www.britannica.com/science/human-renal-system

Located on the medial or concave surface of each kidney is a slit, called the hilus, through which the renal pelvis, the renal artery and vein, the lymphatics, and a nerve plexus pass into the sinus of the kidney. The organ is surrounded by a tough fibrous capsule, which is smooth and easily removable under physiological conditions.

Two distinct regions can be identified on the cut surface of a bisected kidney (Fig. 2): a pale outer region, the cortex, and a darker inner region, the medulla. In humans, the medulla is divided into 8 to 18 striated conical structures, the renal pyramids.

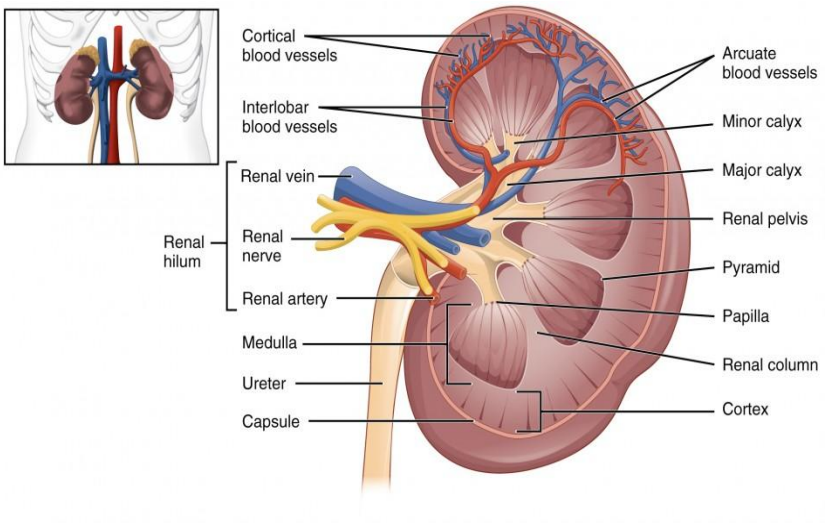

Figure 2: Diagram of the cut surface of a bisected kidney. Extracted from http://www.britannica.com/science/human-renal-system

The base of each pyramid is positioned at the corticomedullary boundary, and the apex extends toward the renal pelvis to form a papilla. On the tip of each papilla are 10 to 25 small openings that represent the distal ends of the collecting ducts (of Bellini). In contrast to the human kidney, the kidney of the mouse and of many other laboratory animals has a single renal pyramid and is therefore termed “unipapillate.” Otherwise, rodent kidneys resemble the human kidney in their gross appearance. In humans, the renal cortex is about 1 cm in thickness, forms a cap over the base of

each renal pyramid, and extends downward between the individual pyramids to form the renal columns of Bertin.

From the base of the renal pyramid, at the corticomedullary junction, longitudinal elements termed the “medullary rays of Ferrein” extend into the cortex. Despite their name, the medullary rays are actually considered a part of the cortex and are formed by the collecting ducts and the straight segments of the proximal and distal tubules.

1.1.2. The nephron

The nephrons are the basic structural and functional units of the kidney (Fig. 3).

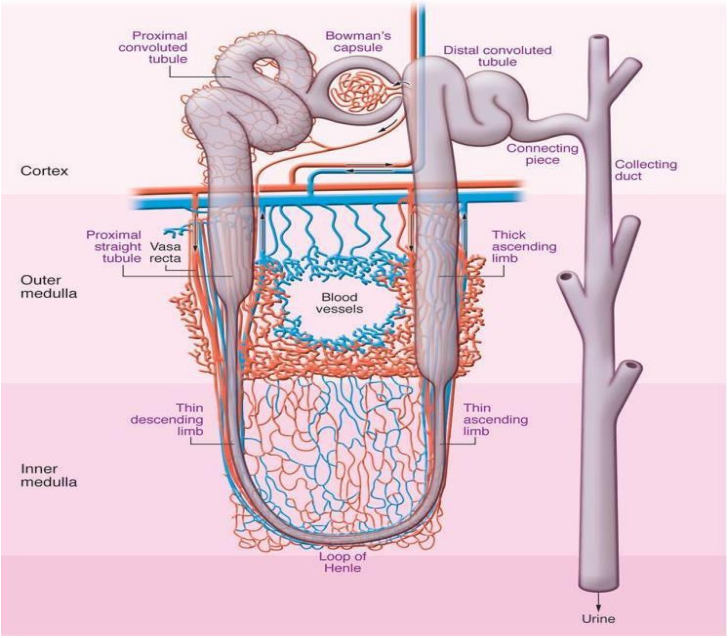

Figure 3: Structure and function of nephron. [2]

Their main function is to regulate water and solute concentration as sodium chloride by filtering the blood, reabsorbing what is needed, and excreting the rest as urine. The nephron also eliminates wastes from the body, regulates blood volume, controls levels of electrolytes and metabolites, and regulates blood pressure pH.

Nephron functions are regulated by hormones such as the antidiuretic hormone, aldosterone, and parathyroid hormone. In humans, a normal kidney contains 800,000 to 1.5 million nephrons. Nephrons span the cortex and medulla. The initial filtering portion of a nephron is the renal corpuscle, which is located in the cortex. This is followed by a renal tubule that passes from the cortex deep into the medullary pyramids. Part of the renal cortex, a medullary ray is a collection of renal tubules that drain into a single collecting duct.

The essential components of the nephron include the renal or Malpighian corpuscle (glomerulus and Bowman's capsule), the proximal tubule, the loop of Henle, the distal tubule, and the connecting tubule [3]. The renal corpuscle filters out solutes from the blood, delivering water and small solutes to the renal tubule for modification. The glomerulus is a capillary tuft that receives its blood supply from an afferent arteriole of the renal circulation. The glomerular blood pressure provides the driving force for water and solutes to be filtered out of the blood and into the space made by Bowman's capsule. The remainder of the blood (only approximately 1/5 of all plasma passing through the kidney is filtered through the glomerular wall into the Bowman's capsule) passes into the efferent arteriole. The Bowman's capsule surrounds the glomerulus. It is composed of a visceral inner layer formed by specialized cells called podocytes.

The renal tubule is the portion of the nephron containing the tubular fluid filtered through the glomerulus. After passing through the renal tubule, the filtrate continues to the collecting duct system, which is not part of the nephron. The components of the renal tubule are:

- Proximal convoluted tubule (lies in the cortex, and is lined by simple cuboidal epithelium with brush border which help to greatly increase the area of absorption).
- Loop of Henle (U-shaped, and lies in medulla)
  - Ascending limb of loop of Henle
  - Descending limb of loop of Henle
- Distal convoluted tubule (a portion of nephron between the loop of Henle and the collecting duct system).

1.1.3. Renal functions

The kidneys participate in homeostasis, regulating acid-base balance, electrolyte concentrations, extracellular fluid volume, and blood pressure. Many of the kidney's functions are accomplished by relatively simple mechanisms of filtration, reabsorption, and secretion, which take place in the nephron. Filtration, which takes place at the renal corpuscle, is the process by which cells and large proteins are filtered from the blood to create an ultrafiltrate that eventually becomes urine. The kidney generates 180 litres of filtrate a day, while reabsorbing a large percentage, allowing for the generation of only approximately 2 litres of urine. Reabsorption is the transport of molecules from this ultra-filtrate into the blood. Secretion is the reverse process, in which molecules are transported in the opposite direction, from the blood into the urine. All the blood in our bodies passes through the kidneys several times a day. The urine is collected in pelvis funnel-shaped structures of the kidneys that drain down tubes called ureters to the bladder.

The 20% of cardiac output is directed toward the kidneys. Most of renal oxygen is utilized to fuel Na^+-K^+-ATPase pumps, which drives tubular sodium reabsorption and other transport processes that are critical for the maintenance of

the physiological homeostasis. Since these transport processes are load dependent, renal oxygen consumption is directly linked to glomerular filtration rate (GFR), which in turn is renal blood flow dependent. In normal conditions, the renal oxygen tension (PO_2) is physiologically low, especially in the medulla, where oxygen tensions of as low as 3 mmHg have been measured. Because of this intricate functional relationship, the kidney operates within a narrow range of relatively constant tissue PO_2, rendering it susceptible to hypoxic injury [4].

1.2.1. Kidney disease: Acute Kidney Injury (AKI)

Kidney disease is an important public health issue and represents a significant and persistent problem in clinical medicine. It is common and its prevalence increases with age, which means that the disease burden will increase with our aging population**.** There is an urgent need to understand the cellular mechanisms behind the development of these pathologies and also to find new effective therapies [5].

Acute kidney injury (AKI) is characterized by a relatively sudden decrease in the production, processing, and excretion of ultrafiltrate by the kidney [decreased glomerular filtration rate (GFR)]. AKI is a syndrome that includes kidney damage from mild injury to total loss of function with seriously implications for fluid homeostasis and electrolyte balance. The Acute Kidney Injury Network (AKIN) defined AKI as "*An abrupt (within 48 hours) reduction in kidney function currently defined as an absolute increase in serum creatinine of more than or equal to 0.3 mg/dl, a percentage increase in serum creatinine of more than or equal to 50%, or a reduction in urine output (documented oliguria of less than 0.5 ml/kg per hour for more than six hours)"* [6].

AKI causes permanent damage to the microvasculature and subsequent abnormalities in kidney structure and function. Through inflammatory and fibrotic signalling pathways, AKI can lead to progressive structural kidney damage, which may then predispose to worsening hypertension, proteinuria, and decline in the glomerular filtration rate (GFR) [7]. AKI can also have long term consequences increasing the risk of developing chronic kidney disease [7]

1.2.2. Incidence

AKI is a common complication in hospitalised patients and presents high morbidity and mortality (30-70%). As a conservative estimate, approximately 17 million admissions a year are complicated by AKI, resulting in additional costs to the health care system of $10 billion just in U.S [7]. In the UK the incidence of AKI is 172 per million per year and the current spending on the managment of AKI is £445 million per year.

The estimated incidence is 3-18% for all hospitalised patients [8] and has increased in the recent years. About two-thirds of patients in intensive care units develop AKI, often as part of the multiple organ dysfunction syndrome. Complications of medical care (9.6%), neoplasms (9.6%), trauma (8.1%), and diseases of the respiratory system (7.9%) comprise large portions of the patients who developed AKI during their hospitalisation. Among the AKI cases, the most common primary discharge diagnosis groups are circulatory diseases (25.4%) and infection (16.4%) [9].

1.2.3. AKI: systemic context

Extra-renal organ dysfunction frequently coexists with AKI, increasing the already high morbidity and mortality rates. Recent experimental models have

elucidated some potential mechanisms of injury, including dysfunctional inflammatory cascades, oxidative stress, activation of pro-apoptotic pathways, differential molecular expression and leukocyte trafficking involved in multisystem diseases. Evidence shows that the AKI is linked with lung, heart, liver and brain dysfunctions (Fig. 4). AKI is frequently associated with respiratory complications and increases mortality in patients with lung diseases. Inflammatory cytokines such as interleukin (IL)-6 and/or IL-8 are potential mediators of renal injury as increase in inflammatory cytokines precede rises in serum creatinine in patients with acute lung injury.

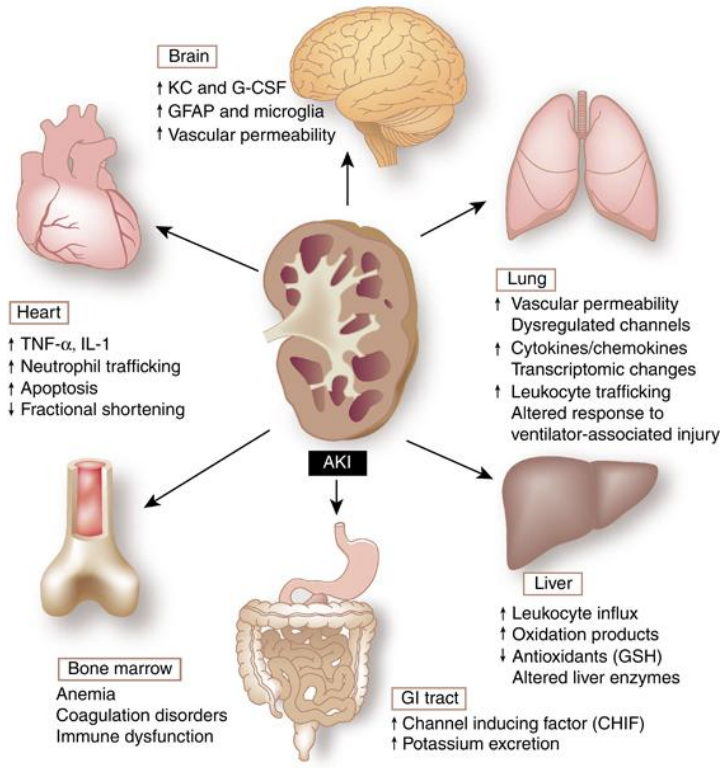

Figure 4: AKI effects on other organs [10]

Patients with established AKI, heart injury has been reported as a common cause of death. Acute cardiac decompensation has effects on the kidney via hemodynamic mechanisms. Also, AKI can lead to myocardial damage as it induces

endothelial cell activation, cytokine secretion, and proapoptotic cascades. Many of the same processes involved in kidney–lung and kidney–heart interactions have been observed in the liver as increased neutrophil infiltration, vascular congestion, and vascular permeability occurs in liver after AKI [10]. Kidney ischemia leads to an elevation of specific liver enzymes such as aspartate aminotransferase, alanine aminotransferase, lactate dehydrogenase as well as bilirubin levels [11]. Neurological complications are recognised in AKI, including central nervous system dysfunction with irritability, attention deficit, hyperreflexia, postural tremor, decreased mental status, seizures and can leads to death. One study reported a connection between AKI and bone marrow and bowel through the release of inflammatory cytokines [11].

1.2.4. Clinical Presentation

Clinical presentation varies with the cause and severity of renal injury, and associated diseases. Most patients with mild to moderate acute kidney injury are asymptomatic and are identified by laboratory testing. Patients with severe AKI, however, may be symptomatic and present with listlessness, confusion, fatigue, anorexia, nausea, vomiting, weight gain or edema. Patients can also show oliguria (urine output less than 400 mL per day), anuria (urine output less than 100 mL per day), or normal volumes of urine (nonoliguric AKI). Other presentations of AKI include development of uruemic encephalopathy (manifested by a decline in mental status, asterixis, or other neurologic symptoms), anemia, or bleeding caused by uraemic platelet dysfunction.

1.2.5. Earlier diagnosis and novel markers

A clinical history and physical examination are crucial for determining early diagnosis and to understand the cause of AKI. The clinical history should identify the use of nephrotoxic medications or systemic illnesses that might cause poor renal perfusion or directly impair in the renal function. Urea and creatinine are nitrogenous end products of metabolism and routinely used in the clinical setting to determine renal function[12]. Urea is the primary metabolite derived from dietary protein and tissue protein turnover. Creatinine is the product of muscle creatine catabolism. Both are relatively small molecules (60 and 113 daltons, respectively) that distribute throughout total body water [13]. Creatinine is a chemical waste product in the blood that passes through the kidneys to be filtered and eliminated in urine. Serum creatinine is widely used measure renal function in renal practice. The well know reciprocal relationship between the serum level and clearance of creatinine in the steady state allows the clinician to estimate renal function from this routinely available measurement [14] .

A blood urea nitrogen (BUN) test measures the amount of nitrogen in blood that comes from the waste product urea.

Discovery of new biomarkers that facilitate the early, sensitive, and specific diagnosis of AKI, is very important to safeguard the health and to prevent haemodialysis and/or transplantation in patients with AKI. The best performing biomarkers allow the diagnosis of AKI within a few hours after an insult, at a time when renal excretory function may still be at baseline, and 24/48 h before serum creatinine levels rise. The availability of well-performing biomarkers will also facilitate more effective testing of new clinical interventions. Surrogate markers of tubular injury are being considered as novel urinary biomarkers for AKI. These markers

include KIM-1 (kidney injury molecule-1) and NGAL (Neutrophil gelatinase-associated lipocalin).

- Kidney injury molecule-1 (KIM-1): KIM-1 is a member of the TIM family which is involved in the regulation of innate and adaptive immune responses [15].

- Neutrophil gelatinase-associated lipocalin (NGAL): Neutrophil gelatinase-associated lipocalin (NGAL) is a protein belonging to the lipocalin superfamily initially found in activated neutrophils. NGAL levels predict the future appearance of acute kidney injury after treatments potentially detrimental to the kidney and even the acute worsening of unstable nephropathies.. Furthermore, recent evidence also suggests that NGAL somehow may be involved in the pathophysiological process of chronic renal diseases [16].

Novel AKI biomarkers, particularly when used in combination panels, possess greater specificity and earlier diagnostic and prognostic sensitivity than serum creatinine and blood urea nitrogen, during both the injury and the recovery phases of AKI [17].

1.3. Etiology of acute kidney injury

The etiology of AKI has traditionally been separated into three categories (Fig.5): prerenal (caused by decreased renal perfusion, often because of volume depletion), intrinsic renal (caused by a process within the kidneys), and postrenal (caused by inadequate drainage of urine distal to the kidneys). In patients who already have underlying chronic kidney disease, any of these factors, but especially volume depletion, may cause AKI in addition to the chronic impairment of the renal function.

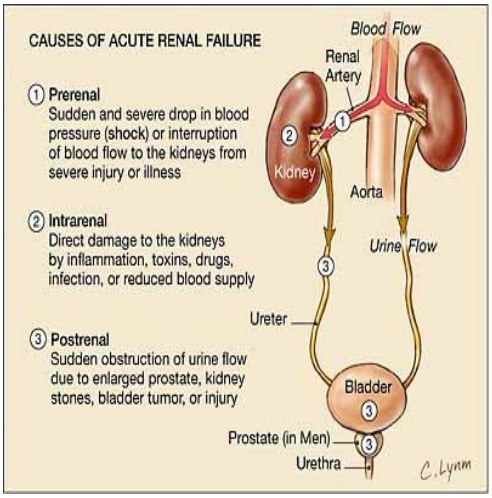

Figure 5: Etiology of AKI.
Extracted from http://www.britannica.com/science/human-renal-system

1.3.1. Pre-renal acute kidney injury

Kidney function may be normal, but decreased renal perfusion associated with intravascular volume depletion (vomiting or diarrhea) or decreased arterial pressure (heart failure or sepsis) results in a reduced glomerular filtration rate. Auto-regulatory mechanisms often can compensate for some degree of reduced renal perfusion in an attempt to maintain the glomerular filtration rate. In patients with pre-existing chronic kidney disease, however, these mechanisms are impaired, and the susceptibility to develop acute/chronic renal failure is higher. Several medications can cause prerenal AKI. Notably, angiotensin-converting enzyme inhibitors and angiotensin receptor blockers can impair renal perfusion by causing dilation of the efferent arteriole and reduce intraglomerular pressure. Nonsteroidal anti-inflammatory drugs also can decrease the glomerular filtration rate by changing the balance of vasodilatory/vasoconstrictive signals in the renal microcirculation. These drugs and others limit the normal homeostatic responses to volume depletion and can be associated with a decline in renal function. In patients with prerenal AKI,

kidney function typically returns to baseline after adequate volume status is established, the underlying cause is treated, or the nephrotoxic drug is discontinued.

1.3.1.1. Pre-renal acute kidney injury: Transplantation

AKI caused by ischemia and reperfusion injury (IRI) is a common event in transplantation, which can contribute to delayed graft function. It is estimated that 20% to 80% deceased donor's kidneys can present delayed graft function (DGF) [18]. Several definitions of DGF have been proposed as: the need of dialysis (at least one session) during the first week post-transplantation, early urine output lower than 1200mL/day or no decrease in serum creatinine within 48 h [19], creatinine clearance lower than 10mL/min and creatinine at day 10 higher than 221µmol/L [20]. A range of factors contribute to DGF such as organ procurement (i.e., kidneys from non heart-beating donors), donor characteristics (i.e., donors older than 55 years), period of ischemia, recipient history (i.e., number of recipient's previous transplants), renal toxicity, ureteral obstruction, among others.

1.3.2. Intrinsic renal acute kidney injury

Intrinsic renal causes of AKI can be categorised by the component of the kidney that is primarily affected (tubular, glomerular, interstitial or vascular). Acute tubular necrosis is the most common type of intrinsic acute kidney injury in hospitalised patients. The cause is usually ischemic (from prolonged hypotension) or nephrotoxic (from an agent that is toxic to the tubular cells). In contrast to a prerenal etiology, AKI caused by acute tubular necrosis does not improve with adequate repletion of intravascular volume and blood flow to the kidneys [21]. Both ischemic and nephrotoxic acute tubular necrosis can resolve over time, although temporary renal

replacement therapy may be required, depending on the degree of renal injury and the presence of pre-existing chronic kidney disease. Glomerular causes of acute kidney injury are the result of acute inflammation of blood vessels and the glomeruli. Glomerulonephritis can be primary a manifestation of a systemic illness (systemic lupus erythematosus) or pulmonary renal syndrome.

Clinical history, physical examination, and urinalysis are crucial for diagnosing glomerulonephritis. Because management often involves administration of immunosuppressive or cytotoxic medications with potentially severe adverse effects, renal biopsy is often required to confirm the diagnosis before initiating therapy [22]. Acute interstitial nephritis can be secondary to many conditions, but most cases are related to medication use, making patient history the key to diagnosis. Acute events involving renal arteries or veins can also lead to intrinsic AKI. Renal atheroembolic disease is the most common cause and is suspected with a recent history of arterial catheterisation, the presence of a condition requiring anticoagulation, or after vascular surgery.

1.3.3. Post-renal acute kidney injury

Post-renal causes typically result from obstruction of urinary flow. Prostatic hypertrophy is the most common cause of obstruction in older men. Prompt diagnosis followed by early relief of obstruction is associated with improvement in renal function in most patients [23].

1.4. Management and treatment of AKI

Optimal management of AKI requires close collaboration among primary care physicians, nephrologists, and other subspecialists participating in the care of the

patient. After AKI is established, management is primarily supportive. Patients with AKI generally should be hospitalised unless the condition is mild and clearly resulting from an easily reversible cause. The key to an correct management is assuring adequate renal perfusion by achieving and maintaining hemodynamic stability and avoiding hypovolemia. There is no specific current treatment for AKI and some patients require renal replacement therapy involving intermittent hemodialysis (IHD) or continuous renal replacement therapy (CRRT). Patients with AKI who require dialysis have a 50–70% mortality rate [24].

1.5. Progression to Chronic Kidney Disease (CKD)

Clinical episodes of AKI may have lasting implications, and new data suggest that these include increasing the chance of subsequent development of CKD. The primary injury leads to reduced flow, which culminates in peritubular capillary loss. This creates a hypoxic environment that produces a fibrotic response that further propagates injury by affecting adjacent unaffected capillaries. Another perspective is that renal injury triggers an inflammatory response that recruits profibrotic cytokines such as transforming growth factor 1 and further induces the transformation of renal epithelial and endothelial cells into myofibroblasts, a process called epithelial or endothelial mesenchymal transition. Myofibroblasts produces excess of extracellular matrix, with subsequent tubulointerstitial injury and atrophy. The histopathological hallmark of CKD is tubulointerstitial fibrosis, and the degree of fibrosis is the best predictor for the progression to end-stage renal disease. In addition to the profibrotic processes, hypoxia also suppresses matrix degradation via reduced expression and activity of matrix metalloproteinases such as collagen metalloproteinase-I. The

eventual loss of the microvasculature creates a hypoxic milieu and produces the progressive nature of fibrosis.

The permanent reduction in peritubular capillary density that occurs following ischemic AKI suggests this leads to a chronic hypoxic state [25].

1.6. Cellular mechanism of AKI

Tubular epithelial cell injury and death with loss of kidney function is common to all types of AKI. It is classical thought that the severity of the injury and the availability of ATP will determine the type of the cell death occurring apoptosis or necrosis. I will further discuss in this section every type of injury.

1.6.1. Nephrotoxic injury

Humans are exposed intentionally and unintentionally to a variety of diverse chemicals that harm the kidneys. Nephrotoxicity results in serious clinical syndromes, including AKI. Nephrotoxic agents have been implicated as etiologic factors in 17%–26% of in-hospital AKI [26]. Drug-induced renal impairment involves many classes of drugs (Tab.1) and includes prescription agents as well as commonly encountered over-the-counter drugs. There are drug-specific and patient-specific risk factors that influence the development of drug-related nephropathy. [26]

Drugs	Use
Vancomycin	Glycopeptide antibiotic
Ciprofloxacin	Fluoroquinolone antibiotic
Penicillins	Antimicrobial agents
Acyclovir	Antiviral agents

Table 1: Drugs that cause AKI

Because renal tubules, especially proximal tubule cells, are exposed to drugs in the process of concentration and reabsorption, they are greatly influenced by drug toxicity [27]. Cytotoxicity is induced by many drugs including aminoglycoside antibiotics, antifungal agents such as amphotericin B, antiretroviral drugs such as adefovir and anticancer drugs such as cisplatin. Nephrotoxic drugs may act at different sites in the kidney, resulting in altered renal function Fig. 6:

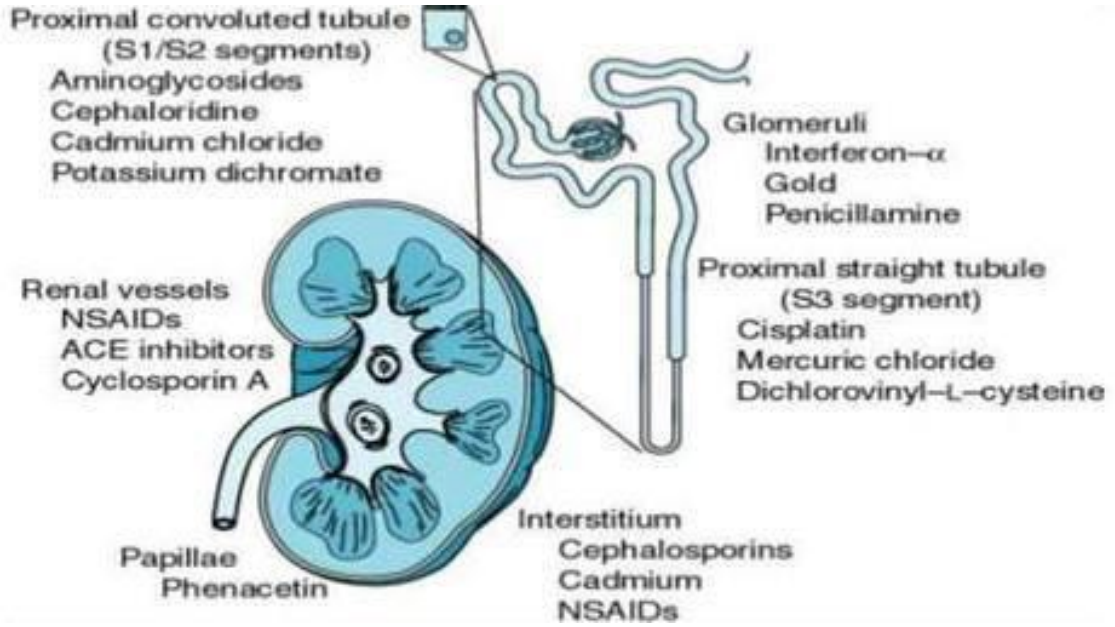

Figure 6: Nephrotoxic drugs act at different sites in the kidney.
Extracted from http://www.britannica.com/science/human-renal-system

The general mechanisms that cause nephrotoxicity include changes in glomerular hemodynamics (NSAIDs and (ACE) inhibitors), tubular cell toxicity, inflammation, crystal nephropathy, rhabdomyolysis and thrombotic microangiopathy[28].

1.6.2. Ischemia reperfusion injury

Renal ischemia/reperfusion injury (IRI), a common cause of AKI, results from a generalised or localised impairment of oxygen and nutrient delivery and waste product removal from kidney cells. There is an imbalance of local tissue oxygen supply and demand and accumulation of waste products of metabolism. As a result, the tubular epithelial cells undergo injury and, if it is severe, cell death. There are many pathophysiological states and medications that can contribute to generalised or localised ischemia (Fig.7) [2].

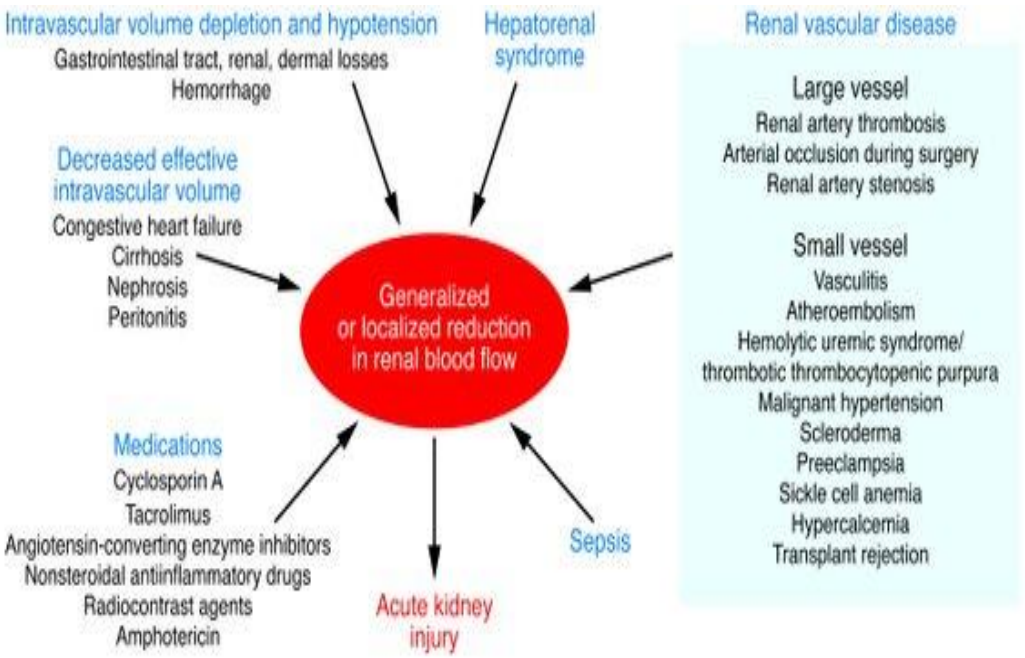

Figure 7: Mechanisms that can lead to ischemia in the kidney. [2]

Alterations in renal perfusion from either hypotension and/or vasoconstriction often lead to clinically significant ischemia. When the duration of ischemia exceeds a certain threshold, intracellular ATP stores become depleted and cells die from either apoptosis or necrosis. While reestablishment of adequate renal perfusion is the main therapeutic goal, rapid re-oxygenation or reperfusion of the ischemic kidney generates additional tissue injury involving multiple mechanisms, such as increased generation of reactive oxygen species (ROS) [29] The mechanisms of AKI involve both tubular and vascular factors.

1.6.2.1 Tubular injury

Ischemia induced AKI is characterised by tubular dysfunction with impaired sodium and water reabsorption and is associated with the shedding and excretion of proximal tubule brush border membranes and epithelial tubules cells into the urine. Tubular damage (Fig.8) that occurs include:

- Loss of epithelial polarity and translocation of Na^+/K^+-ATPase pump from the basolateral membrane into the cytoplasm.
- Proteolytic pathways involving calpains and caspases can participate in proximal tubule cell injury during hypoxia, which may explain the decrease in proximal tubule sodium reabsorption.
- Calcium and ROS production may also have a role in the morphological changes which result in subsequent cell death (necrosis and apoptosis). Both viable and nonviable cells are shed into the tubular lumen, resulting in the formation of casts and luminal obstruction and contributing to the reduction in the GFR. [30]

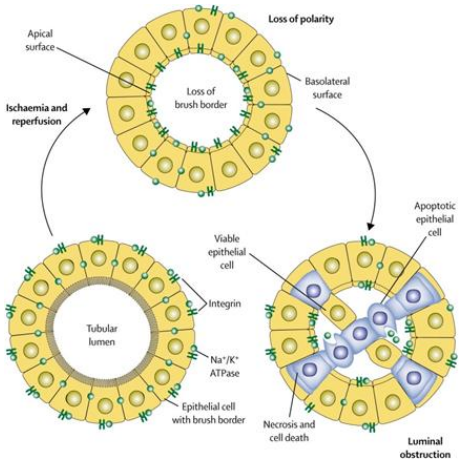

Figure 8: Morphological changes occurring in the proximal tubules following ischemia and reperfusion[32.]

1.6.2.2 Vascular injury

The vascular abnormalities observed in the ischemic kidney may occur as a result of different cellular events:

- Increase in cytosolic calcium in the afferent arterioles of the glomerulus.
- Upregulation of adhesion molecules has been implicated in outer medullary congestion, and antibodies to ICAMs and P-selectin have been shown to afford protection against acute ischemic injury.
- Evidence support that activated leukocytes enhance the renal ischemic injury[30]

1.6.2.3. Cellular mechanism of ischemia reperfusion injury

Renal ischemia-reperfusion injury can be divided in two well differentiated physiological events:

1. Ischemia: adenosine triphosphate (ATP) is provided by glycolysis. However, glycogen stocks are limited and soon are emptied mean while waste products and toxic metabolites including lactate are accumulated. As a result of anaerobic

glycolysis and the hydrolysis of ATP intracellular pH falls. Surprisingly, restoration of a normal pH during reperfusion in ischemic cells accelerates cell death, a phenomenon called the ‘pH paradox’.

2. The reperfusion response can be divided into two distinct phase [31]:
    a Initial phase: During this phase there is an activation of leucocytes that interact with the endothelium inducing inflammation and releasing ROS. They react with the cell membrane causing lipid peroxidation which affects leucocytes and platelets so leading to further vasoconstriction and a reduction in perfusion [32].
    b Later phase: This phase comprises activation of complements and triggering of the innate immunity causing apoptosis and necrosis of the tubular epithelial cells.

1.6.2.4. Tissue repair during IRI

Renal epithelial cells possess a remarkable ability to regenerate and proliferate after IRI (Fig. 9), a quality that is not shared by the majority of other tissues. In the fully developed kidney, cell division is minimal but it can increase more than 10-fold after acute injury. This complex regenerative process involves:

- The first phase consists of cell damage and cell death, during which tubule cells start to generate signals that initiate the regenerative response.
- The second phase is characterised by the appearance of a large pool of de-differentiated epithelial cells with flattened appearance and poorly differentiated brush borders. These cells express vimentin, a marker for multipotent embryonic mesenchymal cells.

- The third phase is exemplified by a marked increase in the number of proliferating tubule epithelial cells that express genes encoding for a variety of growth factors such as IGF-1, HGF, and FGF.
- The fourth phase is one of re-differentiation, during which the normal tubular epithelium is restored with fully differentiated polarized cells. [33]

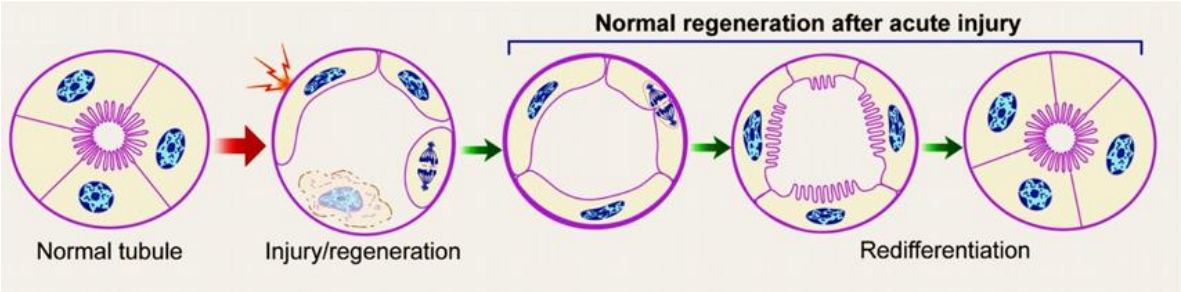

Figure 9: Normal pathway of proximal tubule cell dedifferentiation and proliferation followed by redifferentiation and recovery of normal structure after AKI [34].

1.7. Cell death: apoptosis/necrosis

The balance between cell division and cell death is of utmost importance for the development and maintenance of multicellular organisms. Disorders of either process have pathological consequences and can lead to disturbed embryogenesis, neurodegenerative diseases, or the development of cancer. Therefore, the equilibrium between life and death is tightly controlled. There various types cell death which are executed by active cellular processes that can be intercepted by interfering with intracellular signalling.

1.7.1. Apoptosis

Apoptosis is the major way by which eukaryotes remove superfluous, damaged and other potentially dangerous cells such as malignant cells, virus-infected cells and self-reactive lymphocytes. The process is especially important during development and homeostasis, and is a fundamental process and evolutionaly conserved. Traditionally, cell death has mainly been categorised as apoptotic or necrotic based on morphological changes. The apoptotic cell death process is divided into three phases [35].

- initiation phase (involves the activation of heterogeneous signalling pathways)
- commitment phase (cells become irreversibly committed to death)
- execution phase (morphological changes)

The last step of the apoptosis is characterized by alterations in cellular volume, retraction of pseudopods, chromatin condensation, nuclear fragmentation, plasma membrane blebbing and disassembly of the cell into apoptotic bodies. This process culminates in the engulfment of the apoptotic bodies by other cells, preventing the release of cellular content into the extracellular space. By contrast, necrosis is generally considered an acute and uncontrolled mode of cell death that is associated with cell swelling and lysis, resulting in inflammation in the tissue [36].

1.7.2 Apoptotic signalling pathways

There are two classical signalling pathways leading to the activation of the caspase cascade: the intrinsic and the extrinsic pathways (Fig.10).

- Intrinsic pathway: When the pro-apoptotic signals dominate, the integrity of the mitochondrial membrane is lost in a process known as mitochondrial outer membrane permeabilisation (MOMP). Intrinsic apoptotic stimuli, such as DNA damage or endoplasmic reticulum (ER) stress, activate B cell lymphoma 2 (BCL-2) homology 3

(BH3)-only proteins leading to BCL-2-associated X protein (BAX) and BCL-2 antagonist or killer (BAK) activation and mitochondrial outer membrane permeabilisation (MOMP). Anti-apoptotic BCL-2 proteins prevent MOMP by binding BH3-only proteins and activated BAX or BAK. Following MOMP, release of various proteins from the mitochondrial inter-membrane space (IMS) promotes caspase activation and apoptosis. Cytochrome c binds apoptotic protease-activating factor 1 (APAF1) inducing its oligomerization and thereby forming a structure termed the apoptosome that recruits and activates an initiator caspase, caspase 9. Caspase 9 cleaves and activates executioner caspases, caspase 3 and caspase 7, leading to apoptosis. Mitochondrial release of second mitochondria-derived activator of caspase (SMAC; also known as DIABLO) and OMI (also known as HTRA2) neutralizes the caspase inhibitory function of X-linked inhibitor of apoptosis protein (XIAP). The BCL-2 protein and its homologs are key elements in this regulatory network. The BCL-2 protein family consists of more than 20 proteins divided into three functional groups based on the expression of these BH domains:

- anti-apoptotic BCL-2 proteins (BCL-2, BCL-XL, BCL-W, MCL-1 and A1),
- pro-apoptotic BCL-2 proteins (BAX and BAK);
- pro-apoptotic BCL-2 proteins, (contain the BH3, BH3)

Many of the proteins of the BCL-2 family also contain a trans-membrane domain (TM). The integrity of the mitochondrial outer membrane is tightly controlled by the BCL-2 proteins. Pro-apoptotic members cooperate to induce MOMP, while the anti-apoptotic members preserve mitochondrial integrity. Because the BCL-2 family acts at the mitochondria they are usually upstream of irreversible cellular damage, and therefore these proteins play a pivotal role in whether a cell will live or die.

- The extrinsic pathway to apoptosis is dependent on death receptors belonging to the tumor necrosis factor (TNF) receptor family. Lethal signalling by TNF receptor 1 requires the participation of additional adaptor proteins, including tumor necrosis factor receptor type 1-associated death domain (TRADD). The extrinsic apoptotic pathway is initiated by the ligation of death receptors with their cognate ligands, leading to the recruitment of adaptor molecules such as FAS-associated death domain protein (FADD) and then caspase 8. This results in the dimerization and activation of caspase 8, which can then directly cleave and activate caspase 3 leading to apoptosis. Crosstalk between the extrinsic and intrinsic pathways occurs through caspase 8 cleavage and activation of the BH3-only protein BH3-interacting domain death agonist (BID), the product of which (truncated BID; tBID) is required in some cell types for death receptor-induced apoptosis [37].

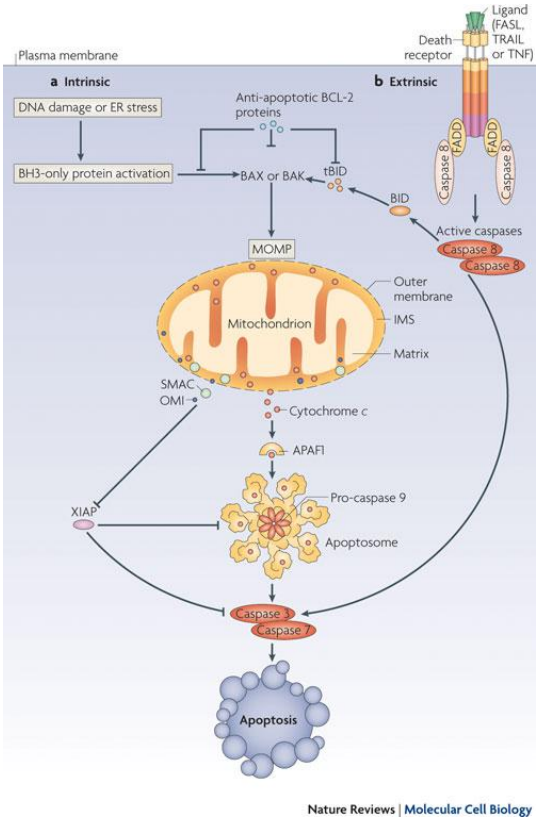

Figure 10: The extrinsic and intrinsic pathways to apoptosis [37].

1.7.3 Necrosis

Necrosis has been traditionally thought to be a passive form of cell death. It is the end result of a bioenergetic catastrophe resulting from ATP depletion to a level incompatible with cell survival and was thought to be initiated mainly by toxic insults or physical damage. Necrosis is characterised morphologically by vacuolation of the cytoplasm, breakdown of the plasma membrane and an induction of inflammation around the dying cell attributable to the release of cellular contents and proinflammatory molecules. Cells that die by necrosis frequently exhibit changes in nuclear morphology but not the organised chromatin condensation and fragmentation of DNA into 200 bp fragments that is characteristic of apoptotic cell death. Figure 11 shows the morphological differences between cells dying by apoptosis and necrosis [38].

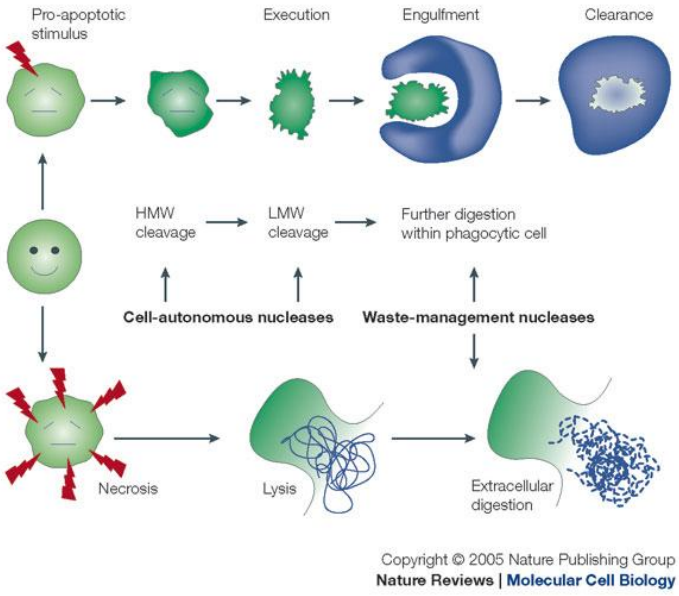

Figure 11: Morphological difference between apoptosis and necrosis [39]

1.7.4. Role of lysosomes in cell death

1.7.4.1. Lysosomes

Lysosomes are single membrane-bound cytoplasmic organelles, present in almost all eukaryotic cells. The shape of the lysosomes varies from spherical to sometimes tubular. Their size differs depending on cell type, and in most cells lysosomes are typically 1 nm. The size and number can increase drastically, for example as a result of accumulation of undigested material. A unique feature of the lysosomal membrane is its high carbohydrate content, due to heavily glycosylated lysosomal membrane proteins [40].They are the major degradative compartment of the endosomal/lysosomal system and the terminal part of the endocytic pathway, where a variety of macromolecules, such as proteins, glycoconjugates, lipids and nucleic acids, are degraded to their building blocks. They are extremely well suited for this function as they contain over 50 different hydrolases. They are further characterized by low pH (3.8-5.0). Among the hydrolases, the proteases, which are responsible for protein degradation, are considered to be highly important.

Although lysosomes are long considered to be responsible primarily for the non-specific degradation of organelles and of the long-lived proteins, it is now clear that they have a number of other functions including selective degradation of proteins, repair of the plasma membrane, release of endocytosed material and removal of certain pathogens. Proteins destined for degradation enter lysosomes via endocytosis (extracellular proteins), phagocytosis (pathogens and cellular debris), micro and macroautophagy (intracellular proteins). Cytosolic proteins can also enter lysosomes via chaperone-mediated autophagy across the lysosomal membrane using heatshock proteins as chaperones and LAMP-2 protein as the receptor that recognizes specific sequences on the target proteins. With the exception of microautophagy and chaperone-mediated autophagy, all other pathways

involve fusion of lysosomes with other vacuoles (phagosomes or autophagosomes) or organelles (late endosomes), indicating that lysosomes are very dynamic organelles [41].

1.7.4.2. Role of lysosomes in apoptotic or necrotic cell death

Most, if not all, cell death pathways eventually lead to lysosomal membrane permeabilisation (LMP), which allows lysosomal content leakage into the cytosol. The high content of hydrolytic enzymes in lysosomes makes them potentially harmful to the cell. Complete or massive lysosomal breakdown induces cytosolic acidification and uncontrolled cell death by necrosis due to indiscriminate degradation of cellular components by lysosomal enzymes. In contrast, partial and selective LMP induces the controlled dismantling of the cell by apoptosis due to lysosomal proteases activity.

Lysosomal proteases that have been implicated in cell death are those cathepsins that remain active at neutral pH, such as cathepsin B, cathepsin D and cathepsin L. Several reports indicate that, in response to some lethal stimuli, not all lysosomes are permeabilised at the same time, although the mechanisms explaining this heterogeneity remain elusive.

Large lysosomes seem to be particularly susceptible to the action of LMP-inducing agents. In addition, the production of intracellular mediators such as ROS, which have a spatially limited range of activity, may induce the permeabilization of lysosomes only in those subcellular regions that are near to mitochondria, the major ROS-generating organelles. Therefore, lysosomes that are localised in the proximity of uncoupled mitochondria are more likely to suffer damage to their membranes than distant lysosomes. Moreover, lysosomes constitute the principal reservoir of chelatable iron, which accumulates upon the autophagic degradation of iron-containing proteins including mitochondrial cytochromes and ferritin. Iron-catalysed Fenton reactions, which produce

highly reactive pro-oxidants, may damage lysosomal membranes. Iron overload, as it occurs in some pathologies and aging processes, can increase the susceptibility of lysosomes to LMP. A second important question regarding LMP is whether it occurs through non-selective rupture of the membrane or whether specific pores are formed that allow for the selective translocation of molecules up to a certain size through the partially permeable lysosomal membrane. In the outer mitochondrial membrane, proapoptotic proteins, BAX and BAK, may form transient pores that allow for the translocation of a number of molecules larger than 100 KDa without inducing a rupture of the membrane, and Bax is also capable of inducing LMP by acting directly on the lysosomal membrane[42].

1.7.4.3 Role of lysosomal cathepsins in apoptosis

The cathepsin protease family consists of 12 known members that can be subdivided into 3 distinct groups, based on the amino acid that comprises the active site residue:

- serine proteases (cathepsins A and G)
- cysteine proteases (cathepsins B, C, H, K, L, S, and T)
- aspartate proteases (cathepsins D and E)

Cathepsins are synthesised as inactive zymogens, and their activation involves proteolytic processing. There are extensive evidences linking cathepsins with apoptosis, in particular cathepsins B and D. In fact, most of the known apoptosis execution pathways occuring in the cytoplasm require translocation of cathepsins that intersect and enhance other apoptosis signalling mechanisms. Cathepsins are released into the cytosol as active enzymes where they can interact with a variety of substrates (BCL-2 family proteins Bid, BCL-2, BCL-XL, and MCL-1, XIAP, caspases-2 and -8, phospholipase A2 (PLA2) and sphingosine kinase-1) contributing to caspase dependent and independent apoptosis with or without mitochondrial involvement. Indeed, in cell culture, apoptosis was found to be

markedly inhibited by Ca074-Me, a specific cathepsin B inhibitor, and by Pepstatin A, a cathepsin D inhibitor [43]. This data confirmed cathepsins B and D, as important components for the apoptosis execution pathways.

Cathepsins are mainly considered to be downstream mediators of lysosomal cells death (LCD), but they can apparently also initiate LMP. In fact, lack of cathepsin B prevents LMP in hepatocytes treated with TNF or sphingosine. The LMP promoting effect of cysteine cathepsins might be due to the intralysosomal degradation of highly glycosylated lysosome-associated membrane proteins, which form a protective glycocalyx shield on the inner lysosomal membrane. Alternatively, minor leakage of cathepsins could activate LMP by cleaving sphingosine kinase 1 or other cytosolic substrates that maintain lysosomal stability. Finally, the activation of apoptotic caspases is frequently associated with secondary LMP that might speed up or amplify the death process. Often, such secondary LMP is initiated by caspase-9, which can be activated in the apoptosome or, in murine cells, by caspase-8-dependent cleavage. After TNF receptor internalization, cathepsin D release can result in activation of caspase-8 and -7- dependent cascade that activates acidic sphingomyelinase, activation of pore-forming BCL-2 proteins (BAX and BAK) and subsequent mitochondrial outer membrane permeabilization (MOMP) [44]. Indeed, in cell culture, apoptosis was found to be markedly inhibited by Ca074-Me, a specific cathepsin B inhibitor, and by Pepstatin A, a cathepsin D inhibitor [43]. This data confirmed cathepsins B and D, as important components for the apoptosis execution pathways.

1.7.4.4. Cathepsin D

Cathepsin-D (CtsD) is a ubiquitous, lysosomal, aspartic endopeptidase that requires an acidic pH (3-4) to be proteolytically active. The human CtsD gene contains 9

exons, and is located on chromosome 11p15. During its transportation to lysosomes, the 52-kDa human pro- CtsD is proteolytically processed to form a 48-kDa, single-chain, intermediate which is an active enzyme located in the endosomes. Further proteolytic processing yields the mature active lysosomal protease, which is composed of both heavy (34 kDa) and light (14 kDa) chains. The human CtsD (Fig.12) catalytic site includes two critical aspartic residues (amino acids 33 and 231) located on the 14-kDa and 34-kDa chains, respectively. CtsD is a key mediator of apoptosis. During apoptosis, mature lysosomal CtsD is translocated to the cytosol due to LMP. Cytoplasmic CtsD can cleave BID to form tBID which triggers the insertion of BAX into the mitochondrial membrane, and leads in turn to the mitochondrial release of Cytochrome c into the cytosol and the activation of pro-caspases 9 and 3 [45]. CtsD is also involved in caspase-independent apoptosis by activating BAX independently of Bid cleavage, and leading in turn to the mitochondrial release of the apoptosis inducing factor (AIF) [46]. More recently, it has been shown that CtsD can also activate pro-caspase 8, initiating neutrophil apoptosis during the resolution of inflammation [47]. In agreement, CtsD inhibitor, Pepstatin A partially delayed the apoptosis induced by different drugs [48].

Since CtsD is one of the lysosomal enzymes that require a more acidic pH to be proteolytically active it is open to question whether cytosolic CtsD is able to cleave the substrate(s) implicated in the apoptotic cascade. In that respect some reports point that CtsD is still active at cytosolic neutral pH, however, its stability is limited due to reversible deprotonation of the active aspartate site. There are several mechanisms that might contribute to prolonged CtsD activity during apoptosis, such as cytosolic acidification or substrate binding.

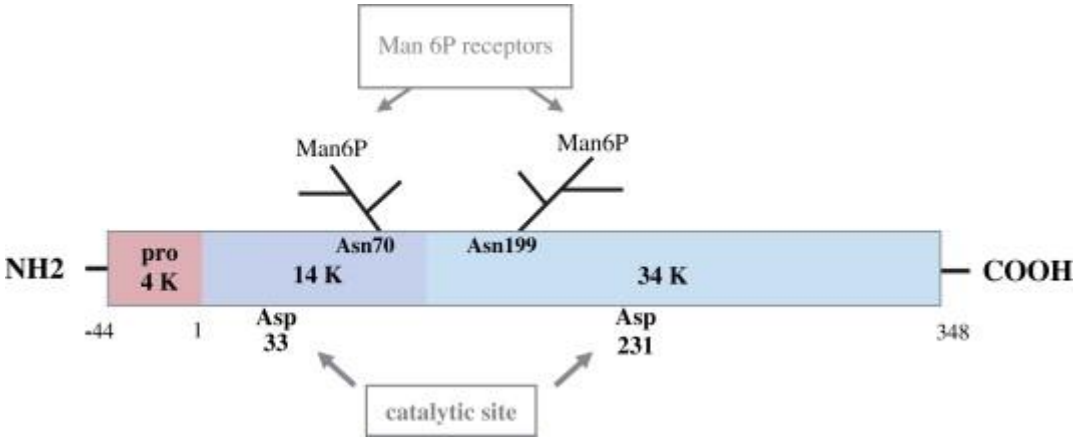

Figure 12: Structure of the human CathepsinD [48].

2 HYPHOTESIS AND AIMS

The role of CtsD in apoptosis is widely supported in the literature [49], however nothing is known about the role of CtsD in apoptosis during AKI. Therefore, my hypothesis is that CtsD plays a role during apoptosis in AKI, and its modulation through inhibitors could have a potential therapeutic beneficial effect.

In order to address this hypothesis, in this thesis I have my addressed 5 main aims:

- Characterisation of CtsD expression in two animal models of AKI, Folic Acid (FA) nephrotoxic model and ischemic reperfusion injury (IRI) model.
- Analysis of the pharmacological inhibition of CtsD over kidney function, tubular cell damage and apoptosis in the two models of AKI.
- Study of the effect of CtsD inhibition in *in vitro* cultured tubular epithelial cells under hypoxic conditions.
- Analysis of the pharmacological of CtsD inhibition on a progressive model of renal fibrosis induced by ischemia reperfusion injury.
- Study of CtsD expression in human acute tubular necrosis transplant patient biopsies.

3 ABSTRACT

Acute kidney injury (AKI) is an abrupt reduction in kidney function due to tubular cell death by toxic or ischemic (IRI) insults. It significantly contributes to graft loss as 20-80% of deceased donor kidneys suffer IRI induced AKI. Despite the progress in the management of the disease, mortality rates in the last five decades remain unchanged at around 50%. Therefore there is an urgent need to find new therapeutic targets against AKI. Lysosomal proteases, particularly CtsD, can play multiple roles in apoptosis, however its role during AKI is still unknown. Here I describe a novel role for CtsD in AKI.

CtsD was upregulated in damage tubular cells in nephrotoxic and ischemic (IRI) induced AKI. CtsD pharmacological inhibition using Pepstatin A lead to an improvement in kidney function, a reduction in apoptosis and an overall decrease in the number of damaged tubular cells in the kidneys with nephrotoxic or IRI induced AKI. Treatment with Pepstatin A slowed progression to CKD from IRI induced AKI, with a reduction in interstitial fibrosis. Analysis of acute tubular necrosis (ATN) transplanted patient biopsies revealed high levels of CtsD in damaged looking tubular cells. CtsD needs to be translocated from the lysosomes into the cytosol to exert its pro-apoptotic function. In agreement with this, CtsD distribution in human disease differed from non-apoptotic to apoptotic cells, with a lysosomal or cytosolic distribution respectively.

My work support the role of CtsD in apoptosis during AKI opening new prospects for the treatment of AKI by targeting lysosomal proteases.

4 MATERIALS AND METHODS

4.1. Reagents and antibodies

Pepstatin A, Folic acid, anti-α-SMA antibody, TriReagent, SYBR Green JumpStart were purchased from Sigma-Aldrich; Cathepsin D (CtsD) activity assay kit, anti-GAPDH and anti-Neutrophil-1 from Abcam; citric acid based antigen unmasking solution, Avidin/Biotin blocking kit, Vectastain Elite ABC Reagent and DAB peroxidase substrate kit from Vector Laboratories; TUNEL In Situ Cell Death Detection Kit, TMR red and DNase I from Roche; Alexa Fluor secondary antibodies and ProLong® Diamond Antifade Mountant with DAPI from Thermo Scientific; Bradford from Biorad; Clearance from Leica; Pig serum from Serotec; Haemalum Mayer from TCS Biosciences; Pertex from Histolab; Pierce ECL reagent and NanoDrop 2000 from Thermo Scientific; X-ray film from Carestream BIOMAX Light Film; Moloney Murine Leukemia Virus Reverse Transcriptase (M-MLV RT) and random primers from Promega; KIM-1 ELISA was from R&D; isopropanol from Fisher Chemical; MTT from Sigma-Aldrich. CtsD antibody was purchased from St Cruz Biotechnolgy; caspase-3 antibody and PARP antibody from Cell Signaling; anti-rabbit biotin conjugated from Dako. Unless otherwise reported all other reagents were from Sigma-Aldrich.

4.2. Animal models

4.2.1. Animal housing and ethics

Mice were housed in the Comparative Biology Centre (CBC) at Newcastle University. Animals were maintained in a 12-h light dark cycle, regulated temperature ($20^{o}C \pm 3\ ^{o}C$) and humidity (50% ± 10%). All the animal studies were done in accordance to the UK Home Office Regulations and under its approval (licence 60/4521).

4.2.2. Drug preparation for *in vivo* use

Pepstatin A was diluted with DMSO to a concentration of 20 mg/mL. For injection 20mg/mL of Pepstatin A stock was diluted 10 times in saline and injected at 10 mg/Kg or 20 mg/Kg. Vehicle was 10% DMSO in saline. Vehicle and Pepstatin A for injection was daily prepared fresh.

Folic acid was diluted in 0.3 M sodium bicarbonate to 25 mg/mL concentration. It was injected intraperitoneally (i.p.) at a concentration of 250 mg/kg. Vehicle was 0.3 M sodium bicarbonate. Both folic acid and vehicle were prepared fresh every time before usage.

4.2.3. Induction of acute kidney injury: Ischemia reperfusion injury (IRI) model

Left renal pedicle of 8-10 week C57BL/6 females was clamped for 25 min. Once the ischemic time was finished, the kidneys were reperfused for 24 h. Controlateral control right kidneys and kidneys from sham animals were used as controls. Sham animals underwent a mock surgical procedure. Vehicle or Pepstatin A (10 mg/Kg) were administered 1 h before surgery and 4 h post-surgery by i.p.injection. Animals were culled 24 h after surgery. A minimum of 7 animals were used in each IRI experimental group [2].

4.2.4. Induction of acute kidney injury: Folic acid (FA) model

A single i.p. injection of 250 mg/Kg of folic acid in vehicle (0.3 M $NaHCO_3$) or vehicle alone was administered to 8-10 week C57BL/6 females. Vehicle or Pepstatin A (20 mg/Kg) were injected i.p. 45 min and 24 h post-folic acid administration. Animals were culled 48 h after folic acid injection. A minimum of 8 animals were used in each folic acid experimental group [26].

4.2.5. Induction of chronic kidney injury: Chronic ischemia reperfusion (IRI) model

In 8-10 week C57BL/6 females the left renal pedicle was clamped for 35 min. Then the clamp was removed, and the kidney was reperfused for 28 days. Sham animals underwent a mock surgical procedure. Vehicle or Pepstatin A (20 mg/Kg) were administered by i.p. injection 1 h before surgery and from day 2 post-surgery three times a week up to 28 days. A minimum of 6 animals were used in each experimental group [34]

4.2.6. Animal sample harvest

4.2.6.1 Blood

The blood from the mice was harvested by cardiac puncture. Cardiac puncture is a suitable technique to obtain a single, large, good quality sample from a euthanized mouse or a mouse under deep terminal anaesthesia. 0.1-1 mL of blood were obtained depending on the size of the mouse and whether the heart was beating. Blood samples were taken from the heart through the diaphragm or the top of the sternum. The blood was collected in eppendorf tubes and it was left to coagulate at room temperature. When the blood was coagulated the samples were centrifuged at 800 r.p.m for 15 min. The serum was collected and transfered into a new eppendorf tube while the pellet was discarded. The samples were stored at -80°C.

4.2.6.2. Urine

Urine were harvested using metabolic cages or single urine spot collection before harvesting. Animals were maintained in the metabolic cages with normal availability of food and water, 12-h light dark cycle, regulated temperature (20°C ± 3°C) and humidity (50% ± 10%. After 24 h the levels of excreted urinary was checked, and the urine were collected on a refrigerated rack (allowing urine collection from +4° down to -15° C).

Then, the urine were centrifuged at 12000 r.p.m. for 15 min to discard possible cell contamination, and the supernatant was stored at -80°C.

4.2.6. Kidney harvest

Kidney harvest was conducted using sterile surgical instruments and consumables (autoclaved), with endeavours to keep the operating area as sterile as possible. The animals were anesthetized with isoflurane. The mice were shaved on the abdomen, placed on their back on a sterilely heated mat, and the limbs were loosely immobilized with sterile masking tape. Then, a 3 cm midline incision in the abdomen to enter the peritoneal cavity was made. A calibri abdominal retractor was inserted. After this step the stomach and the bowel was pulled superiorly to fully expose the kidneys.

The kidneys were isolated from surrounding adventia, fat and the adrenal glands in the peritoneal cavity with fine tip forceps. In the end with fine tipped forceps the kidneys were collected with minimal trauma. The tissues were used for histology, protein and, RNA analysis.

4.3. Biochemical analysis in serum

Blood urea nitrogen (BUN) and serum creatinine assays were performed in serum at the Clinical Biochemistry Department of the Royal Victoria Infirmary, Newcastle.

4.4. KIM-1 ELISA in urine

Mouse KIM-1 microplate were coated with a monoclonal antibody specific for mouse KIM-1. Then, 50 µL of Assay Diluent RD1-55 and 50 µL of Standard and urine were added per well. The microplate was covered with the adhesive strip provided and was incubated for 2 h at room temperature. After this incubation, the solution was aspirated from each well

and washed 3 times with 400 µL washing buffer. After the last wash, 100 µL of cold anti-Mouse KIM-1 Conjugate was added to each well and, the microplate was covered with a new adhesive strip for 1 h at 4 °C, without shaking. After this incubation anti-Mouse KIM-1 Conjugate was removed and washed with 400 µL washing buffer 3 times. Then, 100 µL of substrate solution was added to each well, and the microplate was incubated for 30 min at room temperature. The microplate was kept in the dark. The reaction was stopped by adding 100 µL of stop solution to all the wells. The absorbance was measured using a plate reader at 450 nm with an absorbance correction at 540 nm. The urinary KIM-1 concentration was calculated based on the standard curve and expressed in absolute terms (pg/mL).

4.5. Cell culture of human epithelial tubular cells

4.5.1. Cell maintenance

HKC-8 cells are a cell line derived from human renal proximal tubular, which displays many of the characteristics, such as polarisation and channel expression, of the proximal tubule cells. HKC-8 cells, therefore, are a useful system for the study of human renal proximal tubular cell [50]. HKC-8 cells were cultured in 1:1 Dulbecco's modified Eagle's: F12 medium or DMEM supplemented with 100 U/ml penicillin, 100 µg/ml streptomycin, 2 mM L-glutamine, 5% FBS, and maintained at 37°C at an atmosphere of 20% O_2 /5% CO_2.

The cells cultured were adherent and were routinely grown as a monolayer to approximately 75-100% confluence before passaging.

4.5.2. Cell passage

For passaging cells, the media was aspirated prior to two brief washes in 1x PBS (approximately 10 mL-T75). Cells were then incubated with trypsin-EDTA for 5-15 min. At random intervals during this incubation the detachment of the cells was encouraged by gentle tapping. Once detachment was confirmed by light microscopy, trypsin-EDTA activity was inhibited by the addition of an excess of serum containing media. The trypsin-EDTA/cells mixture was then transferred to a sterile 50 mL Falcon tube prior to centrifugation (typically at 1300 rpm) for 5 min. The supernatant was aspirated off prior to resuspend the cell pellet in fresh media, before seeding the cells as desired for experiment or cell maintenance.

4.5.3. Cell cryopreservation and revival

2.5.3.1. Cryopreservation

Cell lines were frozen down in liquid nitrogen (LqN_2) and at -80°C when no longer required or for stock lines. Cells were detached as outlined in 4.5.2, but the pellet was re-suspended in 5 mL of freezing media [90% (v/v) FCS/ 10% (v/v) DMSO] typically 1-2 mL for a T75 flask before aliquoting into sterile cryovials. The cryovials were then placed into a Nalgene Mr. Frosty Cryo 1°C Freezing Container containing isopropanol, and left at -80°C overnight. This cools the cells at a rate of approximately 1°C per h. The following day, the cryovials were placed in LqN_2.

4.5.3.2. Revival of the cells

Cell were removed from -80°C or LqN2 and rapidly thawed at 37°C in a waterbath, re-suspended in 10 mL freshly warmed media and centrifuged at 1300 r.p.m for five min. The supernatant was then discarded, and the cell pellet re-suspended in 5 mL of fresh

media, which was transferred into two T75 flasks. The cells were left to attach overnight, and the next morning the media was replaced.

4.5.3.3. Cell treatment

HkC-8 cells were seeded in six well plate at a density of 2×10^5 cells/well in 2 mL of DMEM, and left to attach overnight. The next morning the media was replaced with 2 mL fresh warm media, and the cells were treated with Pepstatin A 10mg/mL (final concentration 10 µg/mL) and vehicle (DMSO). The plates were incubated for 48 h at 37°C at an atmosphere of 20% O_2/5% CO_2 (normoxia) or 1% O_2/5% CO_2 (hypoxia). Cell lysates were performed after 48 h of treatment.

2.5.3.4. Cell viability assay (MTT)

The MTT assay is a colorimetric assay for assessing cell metabolic activity. NAD(P)H-dependent cellular oxidoreductase enzymes may, under defined conditions, reflects the number of metabolic viable cells present [51]. The assay was conducted as it follows: HKC-8 cells were seeded in 24-well plates at a density of 1×10^5 cells/well in 1 mL DMEM and were left to attach overnight. The next morning, the medium was removed, and the cells were incubated for 48 h with fresh DMEM with Pepstatin A 10 µg/mL or vehicle (DMSO). The plates were incubated for 48 h at 37°C at an atmosphere of 20% O_2/5% CO_2 (normoxia) or 1% O_2/5% CO_2 (hypoxia). After incubation, MTT reagent (Sigma-Aldrich) (5 mg/mL MTT in PBS) was added to each well being assayed to an equal 1/10 dilution from the original culture volume and incubated for 4 h at 37 °C. After this incubation time, the medium was removed, 1 mL of isopropanol was added, and the absorbance measured at 570nm and 630 nm. The data are expressed as the difference between 630 nm and 570 nm absorbances.

4.6. Histological analysis

4.6.1. Approval for the use human samples

Acute Tubular Necrosis (ATN) transplanted C4b negative biopsy samples were taken under full ethical approval granted by the NRES Committee East Midlands-Derby Research Ethics Committee (REC reference 13/EM/0311), patient consent and in accordance to the approved guidelines.

4.6.2. Immunohistochemistry in mouse and human tissues

4.6.2.1. Cathepsin D immunohistochemistry

Tissue was fixed in 10% formalin for a minimum of 24 h before been processed and embedded in paraffin blocks. Sequential 4μm kidney sections were cut, placed in a water bath set to 45°C, and fixed onto superfrost plus slides (Thermo Scientific). Slides were allowed to cool down and dried overnight at 37°C. Prior to staining, the slides were deparaffinised with Clearene (two washes, 5 min each) and rehydrated through a gradient of alcohol (two consecutive washes of 100% and 70% ethanol solutions, 5 min each). Tissue sections were then incubated in 2% hydrogen peroxide/methanol solution for 15 min to quenching endogenous peroxidase activity. Sections were removed and washed for 5 min in PBS 1X. Then, the sections were incubated for 20 min in a microwave at 750 W with antigen unmasking solution (1/100 in deionised water) (Vector). After cooling with tap water, the sections were mounted into sequence and washed with PBS 1X. Finally, the blocking steps showed in the table 2 were followed. Between every step 3 washes with PBS 1X were performed.

Reagents	Volume	Time
Avidin	3 drops	20 minutes
Biotin	3 drops	20 minutes
Swine Serum	100µL	1 hour

Table 2: Blocking steps.

After blocking, the sections were incubated overnight at 4°C with the primary antibody anti- CtsD (1/100 in swine serum 10%).

After overnight incubation, sections were washed three times for 5 min with PBS 1X. The secondary antibody, anti-rabbit biotin conjugated (1/200 in swine serum 10%) was incubated 1 h at room temperature. After the incubation, sections were washed in PBS for 5 min and 3 drops of ABC regent were added to each section and incubated for 45 min at room temperature. Every section was then incubated with 100 µL of DAB solution (2 drops buffer, 4 drops DAB, 2 drops hydrogen peroxide to 5 mL H_2O) to allow the colour development. The reaction was stopped by rinsing slides with PBS 1X. Following this step, the sections were briefly washed in deionised water before the nuclei were stained with Mayer's Haematoxylin for 60 sec.

Sections were then dehydrated through a series of ethanol solutions for 5 min each (50%, 70%, 100%). Sections were then washed in Clearance twice for 10 min and mounted with Pertex. Slides were dried at room temperature overnight before viewing under a light microscope. Image analysis was performed with a Nikon Eclipse Upright microscope using NIS-Elements BR Analysis software. CtsD human sections staining was assessed by an expert histopathologist. A minimum of 8 different patient biopsies was stained.

4.6.2.2. α-SMA immunohistochemistry

Before the addition of the primary antibody, all the steps were the same as in protocol 4.6.2.1. Sections were incubated overnight at 4°C with the primary antibody anti-α-SMA FITC (1/1500) and wrapped in foil.

After overnight incubation, sections were washed three times for 5 min with PBS 1X. The secondary antibody, anti-fluorescin biotinylated made in goat (1/300 in swine serum 10%) was incubated 2 h at room temperature. After the incubation, sections were washed in PBS for 5 min and protocol was followed as described in section 4.6.2.1.

Slides were dried at room temperature overnight before viewing under a light microscope. Image analysis was performed in a minimum of 10 random 200X fields with a Nikon Eclipse Upright microscope. Using NIS-Elements BR Analysis software, thresholds for α-SMA positive cells area were created, and the analysis was run automatically.

4.6.2.3. NIMP-1 immunohistochemistry

Before the addition of the primary antibody, all the steps were the same as in protocol 4.6.2.1. Sections were incubated overnight at 4°C with the primary antibody anti-NIMP-1 (diluted 1/200). After incubation, sections were washed three times for 5 min with PBS 1X. The secondary antibody, anti-rat biotinylated made in goat (diluted 1/200 in swine serum 10%) was incubated 90 min at room temperature. After the incubation, sections were washed in PBS for 5 minutes and protocol was followed as described in section 4.6.2.1.

Slides were dried at room temperature overnight before viewing under a light microscope. Image analysis was performed in a minimum of 10 random 200X fields with a Nikon Eclipse Upright microscope. Using NIS-Elements BR Analysis software, thresholds for NIMP positive cell area were created, and the analysis was run automatically.

4.7. TUNEL staining

Terminal deoxynucleotidyl transferase dUTP Nick End Labeling (TUNEL) staining is one of the most widely used methods for detecting DNA damage. TUNEL staining relies on the ability of the enzyme terminal deoxynucleotidyl transferase to incorporate labeled dUTP into free 3'-hydroxyl termini generated by the fragmentation of genomic DNA into low molecular weight double-stranded DNA and high molecular weight single stranded DNA [52].

TUNEL was performed in 4 µm paraffin embedded kidney sections. Kidney sections were dewaxed in Clearance for 10 min and rehydrated through a battery of alcohol solutions (100% and 70%). Sections were then washed with PBS 1X for 5 min and incubated in the microwave at 350W with antigen unmasking solution (1/100 in deionised water) for 5 min followed by 1 min at 750W. After a briefly cool down with tap water, the sections were mounted in sequence and washed with PBS 1X. The positive control was incubated with 1000 U/mL recombinant DNase I in 1% BSA for 10 min at room temperature. After this step, the positive control was mounted in sequence and washed with PBS 1X. All the sections were incubated with the blocking solution (3% BSA, 20% Pig serum) for 30 min.

50 µL of Tunnel Reaction Mixture solution (50 µL of enzyme solution + 450 µL label solution) were added on the kidney sections. The negative control received just 50 µL of label solution. The sections were incubated for 1 h at room temperature in a humidified atmosphere in the dark. Finally, the sections were washed with PBS 1X, mounted with ProLong® Diamond DAPi conjugated mounting medium (Invitrogen), and analysed using a Zeiss Axio fluorescent microscope. TUNEL and DAPi positive nuclei were quantified in 10-18 random 200X fields per section using Image J software analysis. Results were

expressed as percentage of the number of positive TUNEL nuclei versus total nuclei (DAPi).

4.8. Dual immunofluorescence TUNEL/CtsD in human paraffin sections

TUNEL staining procedure, described in the paragraph 4.7., was followed until the blocking step with 3% BSA, 20% Piggy serum. After that, anti-cathepsin D (1:100) primary antibody was added overnight in 1% BSA in the cold room. Sections were washed 5 times prior the addition of the anti-goat FITC secondary antibody (1:200) for 1 h at room temperature. From this point, slides were kept in the dark. After washing 5 times with PBS1X, 50 µL of Tunnel Reaction Mixture solution (50 µL of Enzyme solution + 450 µL label solution) was added on the kidney sections. The negative control received just 50 µL of label solution. The sections were incubated for 1 h at room temperature in a humidified atmosphere in the dark. Finally, the sections were washed with PBS 1X and were mounted with ProLong® Diamond DAPi conjugated mounting medium and analysed using a Nikon A1 confocal microscope. Pictures were taken sequentially at 600X oil. 22 images of 0.3 µm slice were acquired per coverslip. Image analysis was performed using Image J software. Images are expressed as merged channels, being each channel the maximum intensity Z stack projection of the 22 individual steps.

4.9. Sirius Red staining

Sirius Red stain is known to specifically bind to collagens due to its sulphonic groups reacting strongly with the basic groups present in collagen molecules. 4µm thick paraffin kidney slides were dewaxed in Clearance and rehydrated through a battery of alcohol solutions (100% and 70%). After this step, the sections were incubated in 0.1%

Sirius Red stain for 2 h at room temperature. Any excess of dye was removed by three brief washes in acidified water (0.5%, v/v) acetic acid in deionised water.

Sections were then dehydrated by incubating them in a series of ethanol solution for 5 min each (50%, 70%, 100%). Sections were finally incubated in Clearance twice for 5 five min each and mounted with Pertex (Histolab). Slides were dried at room temperature overnight before viewing under a light microscope. Image analysis was performed in a minimum of 10 random 200X fields with a Nikon Eclipse Upright microscope. Using NIS-Elements BR Analysis software, thresholds for percentage of positive area was created and the analysis was run automatically.

4.10. Tubular damage assessment and scoring

PAS was performed in 4 µm kidney sections following standard procedures. Tubular damage was assessed in 10-20 random 200X fields in the corticomedullary (CMJ) for the ischemia reperfusion model and the cortex for the folic acid model. Glomerular cast formation was used as an indication of tubular damage in the CMJ and tubular dilation, loss of brush border and epithelial flattening were used as indicators of tubular damage in the cortex. Results were expressed as percentage of the number of damage cells versus total number of cells per field. Using these percentages the score grades were assigned as it follow: score 1 (0-25%), score 2 (25-50%), score 3 (>50%).

4.11. Immunocytochemistry of HKC-8 cells

HKC-8 cells were cultured on glass coverslips in six wells plate, fixed with formalin 10 min, and permeabilized with 0.1% saponine/0.5% BSA for 10 min. After blocking with 3% BSA for 45 min, the coverslip were incubated with anti-HIF1-α antibody for 90 min at room temperature. The coverslips were washed three times with PBS1X between every

step. After washing, secondary anti-mouse-FITC was added and incubated. Coverslips were mounted with ProLong® Diamond DAPi conjugated mounting medium and left to dry overnight at room temperature in the dark. The coverslips were analysed using a Nikon A1 confocal microscope. Pictures were taken sequentially at 600X oil. 3X electronic zoom was made of a region of interest. 10-11 images of 0.75 µm slice were acquired per coverslip. Image analysis was performed using Image J software. Images are expressed as merged channels, being each channel the maximum intensity Z stack projection of the 11 individual steps.

4.12. Protein analysi

4.12.1. Preparation of cellular or tissues lysates

For HKC-8 cells were washed twice with PBS 1X, scrapped in 100 µL of RIPA buffer and transferred into an eppendorf tube. For kidney tissue approximately 50 mg of kidney were homogenised in 1 mL of RIPA buffer. Either cells or tissues were kept in the ice for 15 min and vortex for at least five times to break the cells and release the cellular content. After this step, the cells were sonicated for 5 min in cold deionised water. Supernatants containing cellular lysates were obtained by centrifugation at 14.000 r.p.m for 15 min at 4 °C; pellet containing cellular membranes and nuclei was discarded. The samples were stored at -80 °C.

4.12.2. Protein quantification

Protein samples were quantified with Bradford. The Bradford assay is based on the properties of the Coomassie Brilliant Blue G-250 dye which exists in four different ionic forms. The more anionic blue form binds mostly arginine, tryptophan, tyrosine, histidine, and phenylalanine protein residues, and has an absorbance at 595 nm which can be

measured using a spectrophotometer. Therefore protein concentration can be determined when measured in parallel with a bovine serum albumin (BSA) standard of known concentration.

The Bradford assay was performed in duplicates in 96 well-plate. The proteins samples (1/200) were mixed in 200 µL of 20% Bradford solution and incubated at room temperature for at least 5 min. After this step the plate was read at the spectrophotometer to 595 nm.

The BSA standard curve (Fig 13) was created with concentration plotted on the x-axis and absorbance plotted on the y-axis. This standard curve was then used to determine the concentration of the unknown protein.

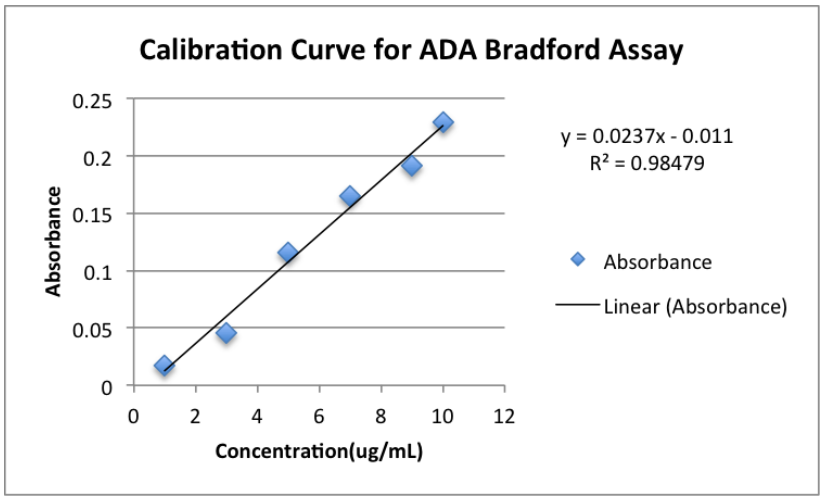

Figure 13: Calibration curve Bradford assay

4.12.3. Electrophoresis sample preparation

10-20 µg of protein were mixed with reducing loading buffer [62.5 mM Tris buffer, pH 6.8, 10% (v/v) glycerol, 2% (w/v) SDS, 100 mM DTT and 0.02% (w/v) bromophenol blue]. Samples were denatured by heating at 90 °C for 5 min. Samples were cold down and centrifuged at 13000 rpm 1 min before loading.

4.12.4. SDS PAGE

SDS-PAGE analysis involves the denaturation of proteins by heating in the presence of both DL-Dithiothreitol (DTT) and SDS (sodium dodecyl sulphate). The combination of these reagents ensures that the protein loses all its secondary, tertiary and quaternary structures and all linear, with a negative charge. Therefore, when loaded onto a gel with fixed pore size, and a current is applied it will migrate towards the positive electrode, governed by its molecular weight. When run against markers of known molecular weight, the molecular weight of unknown protein sample bands could be determined. 8-15% acrylamide resolving gels were set between glass plates clamped together using Biorad system. Gels were prepared according to that reported in the table 3 below:

Resolving gel	**8%**	**10%**	**12%**	**15%**	**Stacking gel**	**6%**
Distilletd water	9.6mL	8.7mL	7.6mL	6.4mL	**Distilletd water**	5.84mL
Tris 1.5 M pH8.8	4.5mL	4.5mL	4.5mL	4.5mL	**Tris 1.5 M pH 6.8**	2.5mL
SDS 10%	180µL	180µL	180µL	180µL	**SDS 10%**	100µL
Acrymalide 40%	3.6mL	4.5mL	5.6mL	6.8mL	**Acrymalide 40%**	1.5mL
APS 10%	90µL	90µL	90µL	90µL	**APS 10%**	50µL
TEMED	18µL	18µL	18µL	18µL	**TEMED**	10µL

Table 3: Acrylamide gels receipt.

A thin layer of isopropanol was applied to remove air bubbles and ensure a level interface between the stacking and separating gels. Upon polymerisation the isopropanol was removed before the stacking gel was cast on top. The stacking gel was prepared according table 3. Combs were carefully placed into the stacking gel to form the wells for the samples to be loaded into. When polymerisation was complete the combes were

removed, and the gels were fastened into the gel tank, which was then filled with electrode running buffer (1x ERB) (20 mM Tris, 160 mM glycine and 0.08% (w/v) SDS, pH 8.3). 10-20 µg total proteins was loaded per well. Electrophoresis was carried out at 80 V initially until the dye front had crossed the interference of the stacking and resolving gel. After that, the voltage was increased to 120V until the dye front had reached the end of the gel. At this point the gels were removed from the tank and the Western blotting was performed according to the next paragraph.

4.12.5. Western blotting

After the electrophoresis, the stacking gel was discarded whilst the resolving gel was placed in chilled transfer buffer [25 mM Tris, 192 mM glycine and 20% (v/v) methanol, pH 8.3]. Gels were loaded into the Western transfer cassettes overlayed with the nitrocellulose membrane between both filter paper and pads, and placed into the tanks with ice pack before being immerged in chilled transfer buffer (Fig 14).

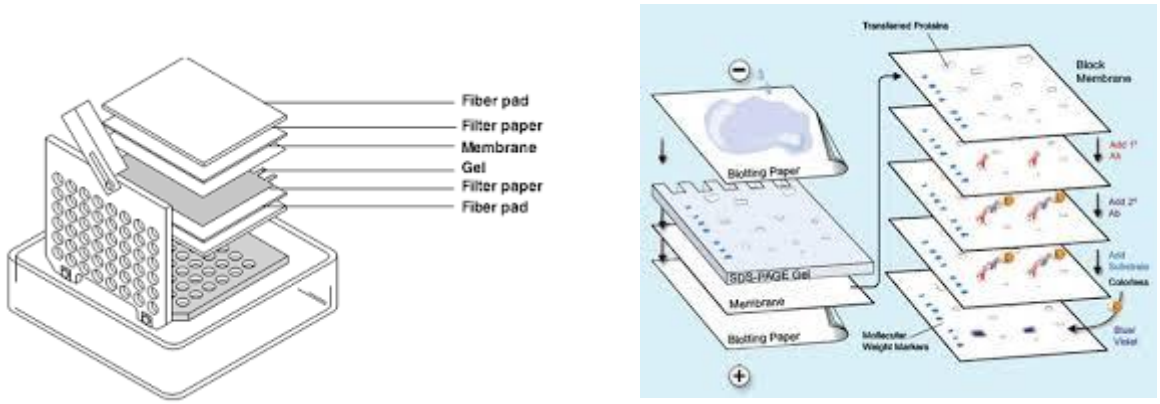

Figure 14: Western transfer picture representation.

he negatively charged proteins were transferred onto the positively charged nitrocellulose membrane by running the tank at 290 mA for 1 h. Afterwards, the nitrocellulose membrane was removed and washed in 1x TBS-T [0.2 M NaCl, 20 mM Tris

and 0.05% (v/v) Tween 20, pH 7.4] to remove any traces of methanol. The nitrocellulose membrane was then then blocked in 3% (w/v) marvel milk powder in 1X TBS-T buffer for 1 h at room temperature to prevent non-specific protein binding.

The nitrocellulose membrane was then washed three times in 1X TBS-T, prior to incubation with the primary antibodies (Tab.4) diluted in incubation buffer (0.3% (w/v) milk powder in 1X TBS-T) overnight at 4 °C.

Antibody	Dilution	MW (KDa)	Reference number	Supplier
Goat polyclonal Anti-cathepsinD	1/250	46	sc-6486	St Cruz Biotechnolgy
Rabbit monoclonal Anti-cleaved Caspase-3	1/1000	19	5A1E	Cell Signaling
Goat polyclonal Anti-GAPDH	1/1000	37	ab9483	Abcam
Rabbit monoclonal PARP Antibody	1/1000	89	9542	Cell Signaling

Table 4: Primary WB antibody list.

Following three 1X TBS-T washes, the membrane was incubated with the appropriate secondary antibodies for 1 h at room temperature. Finally, the membrane was washed for a minimum of 30 min with multiple TBS-T changes prior to chemiluminescent detection.

4.12.6.Protein chemiluminescent detection

Pierce ECL reagent was used for chemiluminescent detection of the horseradish peroxidase (HRP) activity of the intended protein. Following the guidelines provided, equal volumes of reagents 1 and 2 were mixed and pipetted onto the membrane, ensuring that it was covered equally for 1 min. Excess ECL reagent was removed by blotting with tissue paper. The membrane was fixed into a cassette, and exposed to X-ray film in a dark room followed by development of X-ray film with a Xograph SRX-101A developer.

4.12.7. CtsD activity assay

Cathepsin D (CtsD) activity was determined using CtsD activity assay kit which is a fluorescence-based assay that utilizes the preferred CtsD substrate sequence GKPILFFRLK(Dnp)-D-R-NH2) labelled with 7-methoxycoumarin-4-acetic acid (MCA). The CtsD contained in the samples cleaves the synthetic substrate releasing fluorescence, which can be quantified using a fluorescence plate reader.

10 µg of proteins were incubated with the lysis buffer up to 50 µL of final volume for each sample in the 96 wells black plate. 52 µL of reaction mix (50 µL reaction buffer + 2 µL substrate) were added in each well. Plate was then read to obtain the basal reading and incubated at 37°C. Readings were done after 1 and 2 h using a fluorescence plate reader at Ex/Em = 355/520 nm. Results are expressed as a slope of fluorescence emission after 1 h or 2 h per µg of protein.

4.13. Gene expression analysis

4.13.1. RNA Isolation

Kidney tissue was homogenised in 1 mL of TriReagent in an RNase/DNase free eppendorf. 200µL of chloroform were added and mixed carefully prior to centrifugation at

13,000 rpm for 15 min at 4°C. The upper aqueous layer containing the RNA was removed and transferred to a new tube. Then, 500 µL chilled sterile isopropanol were added, and the mixture was incubated on ice for 20 min; before centrifugation at 13,000 rpm for 10 min at 4°C. The supernatant was discarded, and the RNA pellet washed in 500 µL 70% ethanol (diluted in sterile water nucleasi-free) before a final 10 min centrifugation step at 13,000 rpm at 4°C. Finally, following removal of the 70% ethanol, the RNA pellet was left to dry and was re-suspended in a small volume (typically 10-30 µL) of nuclease free water dependent upon the pellet size. The purified RNA was quantified by NanoDrop 2000.

4.13.2. cDNA synthesis

Moloney Murine Leukemia Virus Reverse Transcriptase (M-MLV RT) is an RNA-dependent DNA polymerase that can be used in complementary DNA (cDNA) synthesis with long messenger RNA templates.

1 µL of RNA at 500 ng/µL was added to 8 µL of RNase free water plus 1 µL of DNase and 1 µL of DNase buffer. This mix was incubated for 30 min at 37°C. Then, 1 µL of DNase stop solution was added to stop the reaction, and the mix was left at room temperature for 2 min. After this step, 0.5 µL of random hexamer and 2 µL nuclease free water were added, and the mix was incubated at 70°C for 5 min. The mix was kept in ice prior to add 6.5 µL of Retro transcription mix (Tab.5). The samples were than incubated for 1 h at 42°C to produce 1st strand cDNA, and stored at -20°C.

RNAsin	0.5µL
MMLV RT buffer	4 µL
MMLV RT	1 µL
dNTPs	1 µL

Table 5: Retrotranscription mix

4.13.3. Primer design and sequences

Primers sequences were obtained from the Primers Bank of Harvard Medical School (http://pga.mgh.harvard.edu/primerbank/). The gene accession number for the mRNA of interest was found on NCBI database in the sections Nucleotide (http://www.ncbi.nlm.nih.gov/pubmed). The gene accession was inserted in the Primer Bank and chosen primers were run in BLAST (http://blast.ncbi.nlm.nih.gov/Blast.cgi), to check for unspecific binding of the selected primers. All the sequences are reported below (Tab.6).

Gene (GenBank Accession)	**Primer sequence**
Col1A1 (NM_007742)	Fw: 5'-TTCACCTACAGCACGCTTGTG-3'
	Rv: 5'-GATGACTGTCTTGCCCCAAGTT-3'
Col 3A1 (NM_009930)	Fw: 5'-CTGTAACATGGAAACTGGGGAAA-3'
	Rv: 5'-CCATAGCTGAACTGAAAACCACC-3'
CXCL-1 (NM_008176)	Fw: 5'- CTGGGATTCACCTCAAGAACATC-3'
	Rv: 5'- CAGGGTCAAGGCAAGCCTC-3'
CXCL-2 (NM_009140)	Fw: 5'- CCAACCACCAGGCTACAGG-3'
	Rv: 5'- GCGTCACACTCAAGCTCTG-3'
IL-1β (NM_008361)	Fw: 5'-CAACCAACAAGTGATATTCTCCATG-3'
	Rv: 5'-GATCCACACTCTCCAGCTGCA-3'
IL-6 (NM_031168)	Fw: 5'- TAGTCCTTCCTACCCCAATTTCC-3'
	Rv: 5'- TTGGTCCTTAGCCACTCCTTC-3'
RANTES (NM_013653)	Fw: 5'-TGCTGCTTTGCCTACCTCTCC-3'
	Rv: 5'- TGGCACACACTTGGCGGTTCC-3'

TNF-α (NM_013693)	Fw: 5'-CCCTCACACTCAGATCATCTTCT-3'
	Rv: 5'- GCTACGACGTGGGCTACAG-3'

Table 6: Mouse primers sequences.

4.13.4. Quantitative real-time PCR (qRT-PCR)

cDNA samples were diluted up to 10 ng/µL. 20 ng of cDNA was added per reaction. Samples were run in duplicate. 18 µL of SYBR green mastermix (Tab.7) were added to each well in turn.

DNase free water	6µ
2X SYBR Green (Sigma-Aldrich) JumpStart	10µ
Primer reverse	1µ
Primers forward	1µ

Table 7: SYBR green mastermix

The plate was run on an Applied Biosystems 7500 Fast Real-Time PCR system machine; after the initial denaturation step, there were 40 repeated cycles consisting of95°C for 5 sec,60 or 55°C for 30 sec,72°C for 1 min.

The level of SYBR Green JumpStart detected was measured during the cycling step of each cycle, and the cycle threshold (C_T) values were calculated by manually applying a threshold limit to represent the exponential phase of the amplification. SYBR Green binds to double strand DNA (dsDNA) and the fluorescence was detected at the end of each elongation step giving a value to the amount of dsDNA present.

Quantitation of gene expression was calculated relative to the housekeeping control 18S using the comparative ΔΔCt method. Briefly, the mean and standard deviation (SD) of the C_T values were calculated for 18S and the target gene. The ΔC_T was calculated by subtracting the 18S C_T from the target gene C_T. Data were plotted against vehicle sham or control group.

4.14. Statistical analysis

Results are expressed as mean ± SEM unless otherwise stated in the figure legend. All p values were calculated using student's t-test. $^{*}P \leq 0.05$, $^{**}P \leq 0.01$ or $^{***}P \leq 0.001$ was considered statistically significant.

5. RESULTS

5.1. Characterization of CtsD expression in folic acid (FA) induced nephrotoxic AKI

Nephrotoxic AKI can happen due to a wide variety of commonly used drugs [2]. Intrinsic damage into the kidney tissue will lead to cell death contributing to the decline in kidney function and the development of AKI. First of all, I analysed the expression of CtsD, through Western blotting (WB) and immunostaining in the nephrotoxic AKI model of FA injection. Administration of high doses of FA induces acute tubular necrosis by crystal formation mainly within the cortical area [44]. 8-10 week C57BL/6 females were given a single i.p. injection of 250 mg/Kg of FA in vehicle (0.3 M $NaHCO_3$), or vehicle alone. The animals were culled after 48 h of the injection and the kidneys were collected.

Figure 15A shows CtsD WB in the kidney lysates from vehicle and FA treated mice 48 h after injection. For this WB 20 µg of total kidney protein was loaded per well. Pro- (52KDa) and mature (48KDa) forms of CtsD protein were increased in mice treated with FA compared with mice treated with vehicle. This data suggests that CtsD could be involved in nephrotoxic AKI. GAPDH protein expression was unchanged and used as the WB loading control (Fig. 15A).

WB resultes were confirmed by CtsD immunostaining in kidney tissue. Paraffin embedded kidney tissues were stained for CtsD as described in the methods section 4.6.2.1. CtsD staining in kidney cortex confirmed an increase of CtsD expression mainly in damaged tubular epithelial cells in the mice treated with FA. Almost no expression of CtsD was detected in the cortex from non-injured mice (Fig. 15B). These data confirmed that CtsD is upregulated in FA induced nephrotoxic AKI.

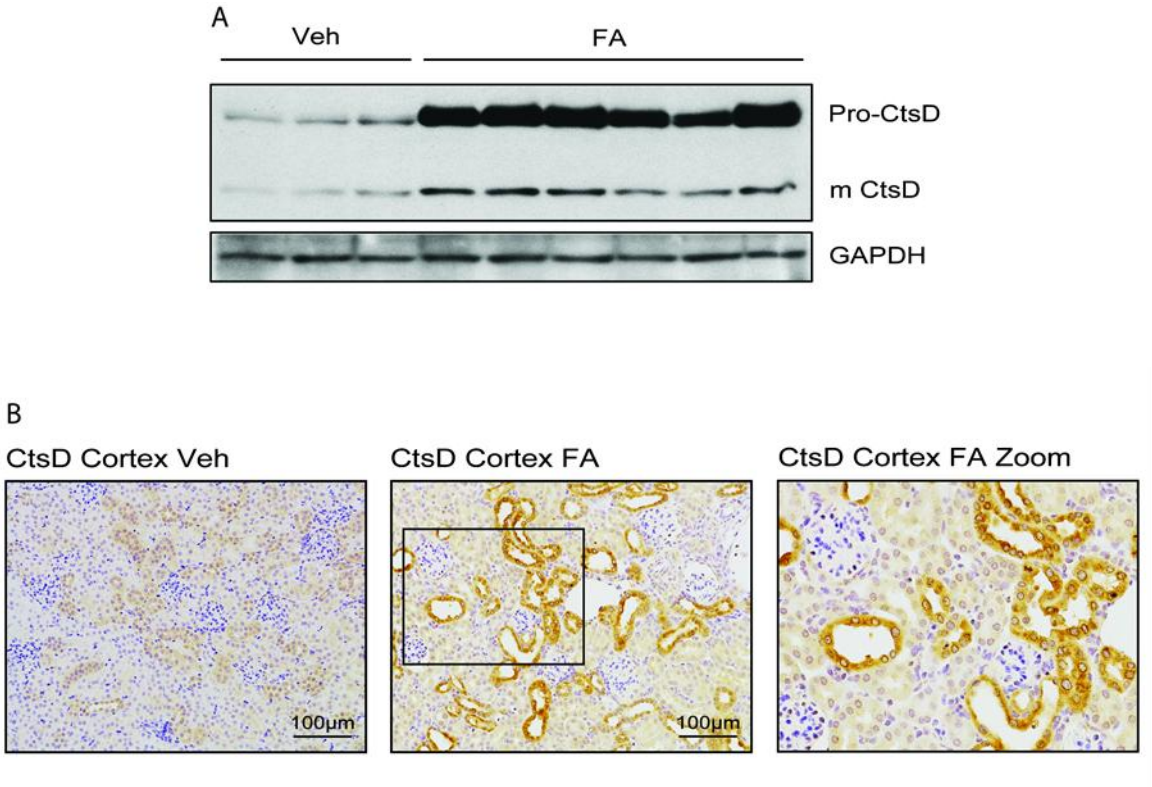

Figure 15: Western Blot of pro- and mature form of CtsD and GAPDH in total kidney lysates **(A)**. Representative pictures of CtsD cortical immunostaining(beown) of kidney tissue **(B)**. Animals were treated with FA (250mg/Kg) or vehicle for 48 h.

5.2. Effect of pharmacological inhibition of CtsD by Pepstatin A in a FA induced nephrotoxic AKI model

To understand the role of CtsD in FA nephrotoxic induced AKI, the CtsD inhibitor Pepstatin A was administrated. Pepstatin A (20 mg/Kg) was injected i.p. 45 min and 24 h post-FA administration. A minimum of 8 animals was used in each FA experimental group. The control animals were injected with vehicle alone. After 48 h of FA administration the animals were culled and blood, urine and kidneys collected. The results obtained are listed below.

5.2.1. Effect of CtsD inhibition on kidney function during FA induced AKI

Kidneys functions was assessed using biomarkers on the serum and urine. The biochemical markers blood urea nitrogen (BUN) and creatinine were analysed in serum (Fig 16A and 16B). As expected, both markers were increased upon FA administration compared with vehicle. Interestingly, animals receiving both FA and Pepstatin A treatment had a significantly lower BUN and creatinine concentration than the ones which received FA and vehicle, reflecting improved kidney function (Fig 16A and 16B).

Moreover, the urine biomarker KIM-1 was used to determined renal tubular injury (Fig 16C). In agreement with the serum results, urine KIM-1 was increased in AKI induced by FA but was lower in the animals treated with Pepstatin A compared with the ones treated vehicle alone.

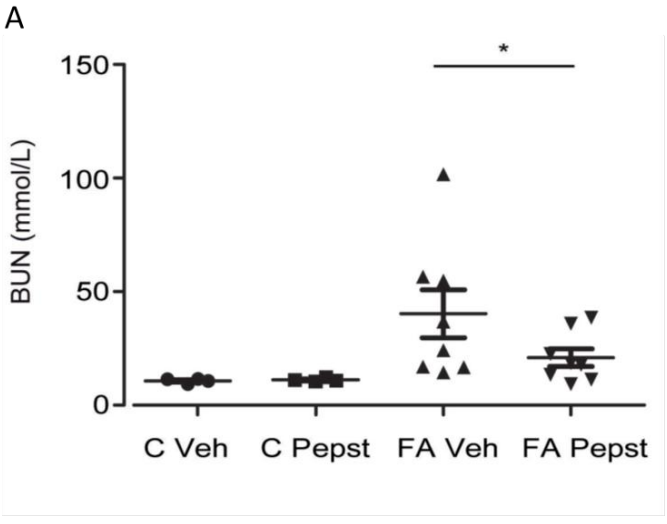

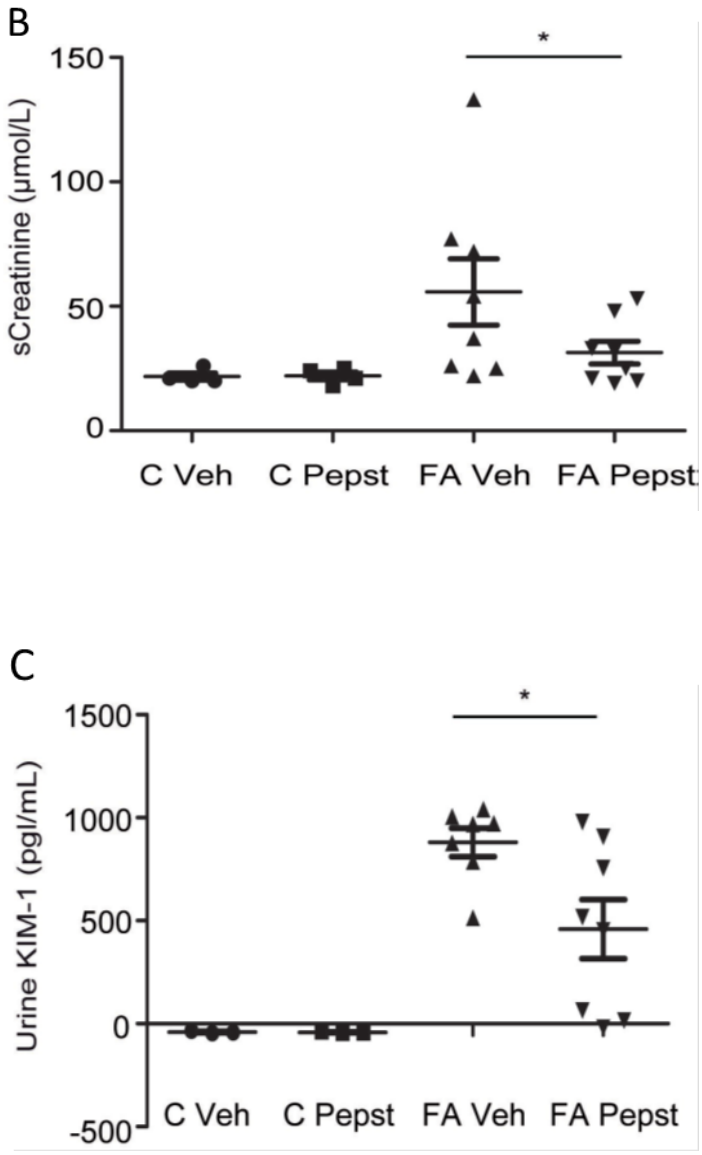

Figure 16: BUN (**A**), serum creatinine (**B**), urine KIM-1 ELISA (**C**) in control and 48 h FA vehicle and Pepstatin A treated kidneys. Animals were treated with vehicle or Pepstatin A (20mg/Kg) 45 min before and 24 h post-FA. Repeated measures t-test, *P ≤ 0.05

5.2.2. Effect of Pepstatin A on tubular cell damage during FA induced AKI

To determine the real tubular cell damage PAS staining and scoring was performed. Damaged tubules were classified according to previously described AKI clinical pathological description using the following criteria: tubular dilation, loss of brush border and epithelial flattening. Tubular damage was assessed in 10-20 random 200X fields in the cortex.

Analysis of kidney tissues from FA vehicle or Pepstatin A treated mice showed that Pepstatin A reduces by 40% the percentage of tubular cell damage in FA treated animals (Fig. 17A). In agreement, the histomorphological injury score was also significantly reduced by Pepstatin A treatment (Fig. 17B). The improvement in kidney function and a decrease on the tubular cell damage in Pepstatin A treatment could be explained by a direct effect of CtsD inhibition on inflammation [53] or on epithelial tubular cell death [54].

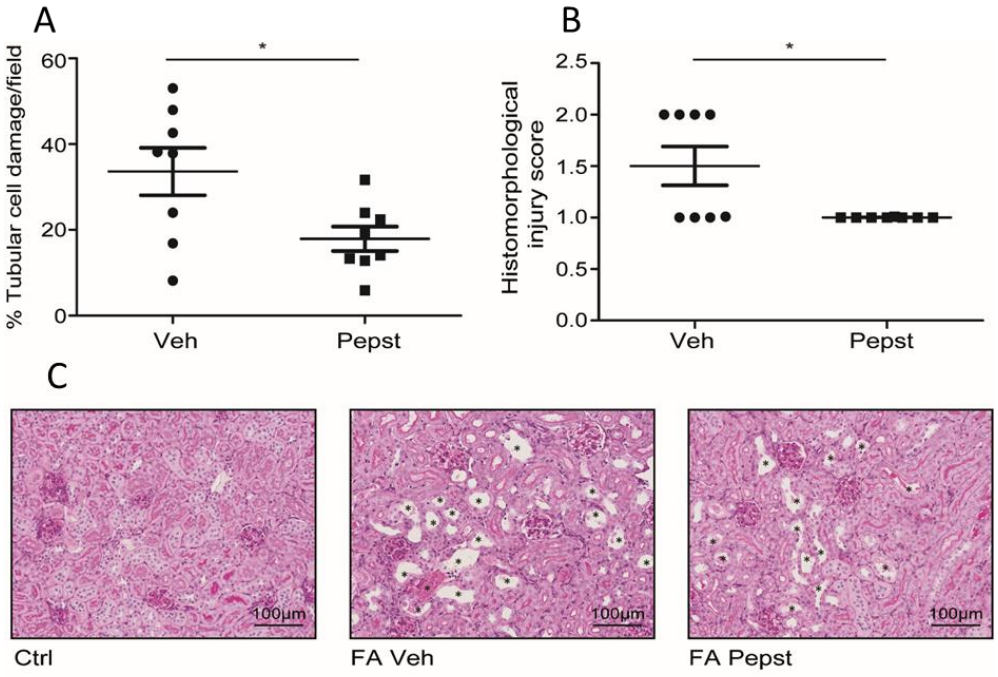

Figure 17: Percentage of tubular cell injury in cortex **(A)** or histomorphological injury score (**B**) as assessed by tubular dilatation, epithelial flattening and loss of brush border in FA vehicle or Pepstatin A treated kidneys. Representative PAS pictures **(C)**, damaged tubules *. Animals were treated with vehicle or Pepstatin A (20mg/Kg) 45 min before and 24 h post-FA. Repeated measures t-test, *P ≤ 0.05

5.2.3. Effect of CtsD inhibition on kidney inflammation during FA induced AKI

To clarify the role of CtsD in inflammation during AKI, gene expression of inflammatory mediators was analysed by RT-PCR. The inflammatory mediators analysed were CXCL-1, CXCL-2, IL-1β, lL-6, TNF-α and RANTES [55], and the results

are shown in figure 18. The expression of all the inflammatory mediators was significantly increased in the mice that were treated with FA. Pepstatin A did not influence on their expression apart from the expression of IL-1β that was significantly decreased.

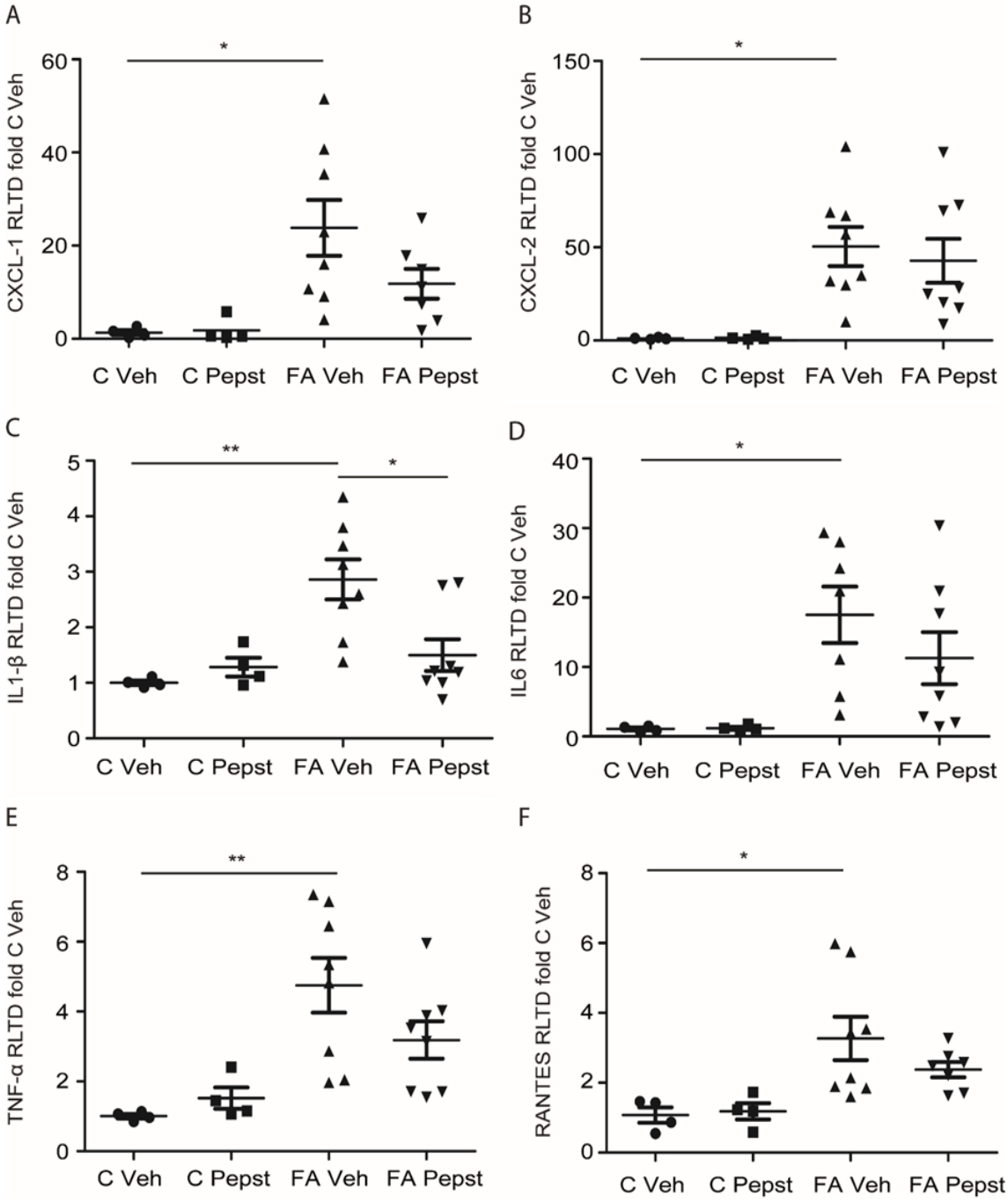

Figure 18: CXCL-1 **(A)**, CXCL-2 **(B)**, IL1-β **(C)**, IL-6 **(D)**, TNF-α **(E)** and RANTES **(F)** mRNA expression from control and 48 h FA vehicle or Pepstatin A treated kidneys. Animals were treated with vehicle or Pepstatin A (20mg/Kg) 45 min before and 24 h post-FA. Repeated measures t-test, *P ≤ 0.05 or **P ≤ 0.01

5.2.4. Effect of Pepstatin A on apoptosis during FA induced AKI

Next I determined the effect of Pepstatin A on apoptosis by two different methods. First of all, apoptosis was evaluated through WB of active-caspase 3, an effector apoptotic caspase. The extrinsic apoptotic pathway is initiated by the ligation of death receptors (TGF) with their cognate ligands, leading to the recruitment of adaptor molecules such as FAS-associated death domain protein (FADD) and then caspase 8. This results in the dimerisation and activation of caspase 8, which can directly cleave and activate caspase 3, leading to apoptosis [37]. Control kidney treated only with vehicle was compared with FA kidneys treated with vehicle or Pepstatin A. FA administration increased cleaved or active caspase-3 in kidney tissue and increase that was inhibited by Pepstatin A administration indicating a reduction in apoptosis due to CTsD inhibition. GAPDH protein expression was unchanged and used as the WB loading control (Fig. 19A).

In order to confirm the effect of Pepstatin A on apoptosis induced by FA, TUNEL staining was performed. TUNEL staining (Fig 19B) confirmed WB data showing a 50% reduction in the percentage of apoptotic positive cells in the FA injury kidneys of mice treated with Pepstatin A compared with vehicle. In the control kidneys, TUNEL positive cells were not detected. Therefore, CtsD inhibition improves kidney function, reduces tubular damage and apoptosis in FA nephrotoxic induced AKI model.

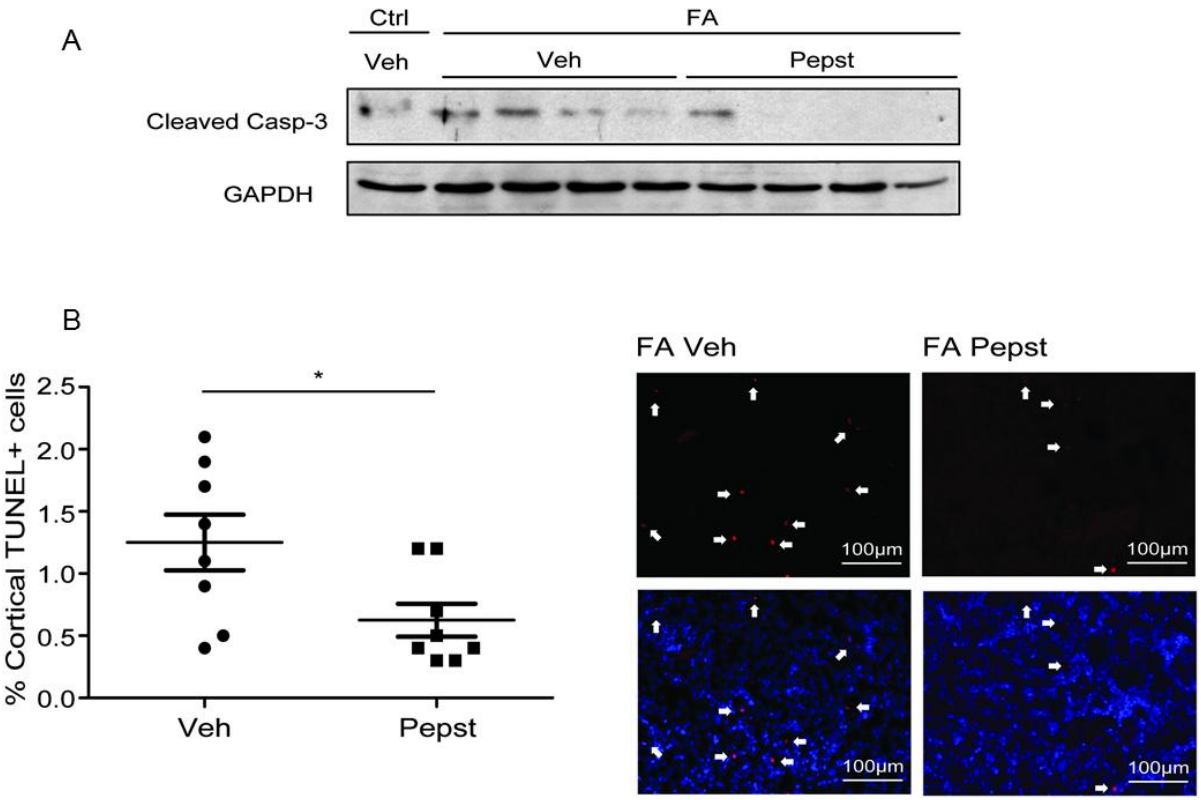

Figure 19: Cleaved caspase-3 and GAPDH WB **(A)**. Percentage of cortical TUNEL positive cells versus total cells and representative TUNEL +/- DAPI pictures **(B)** in FA vehicle or Pepstatin A treated kidneys. White arrows point to TUNEL^{+} cells. Animals were treated with vehicle or Pepstatin A (20 mg/Kg) 45 min before and 24 h post-FA. Repeated measures t-test, *P ≤ 0.05

5.3. Characterisation of CtsD expression and its correlation with the levels of apoptosis in ischemia reperfusion induced AKI

AKI can be induced by many conditions, in this thesis two models were evaluated, FA and IRI. Both necrosis and apoptosis contribute to tubular loss during IRI [56]. The cell death ratio biases towards necrosis rather than apoptosis as the severity of the damage increases with higher ischemic times [57]. Thus, I first characterised the contribution of apoptosis to a mouse model of renal IRI. I performed different ischemic times (25, 35 and 45 min) with the same reperfusion time (24 h). After 24h the animals were culled and blood, urine and kidneys were

collected. Contralateral right kidneys and kidneys from sham animals were used as controls. Sham animals underwent a mock surgical procedure. The effect of different ischemic times on apoptosis was analysed by WB of selected apoptotic markers. I chose two well described apoptotic events, the cleavage of the effector caspase-3 and the inactivation or cleavage of Poly ADP ribose polymerase-1 (PARP-1). PARP-1 is an enzyme participating in DNA repair which contributes to apoptosis by caspase-3 inactivation or cleavage [58]. Both, active caspase-3 and caspase dependent cleaved PARP-1 fragment were increased after 25 min of ischemia in comparison with the control kidneys (Fig. 20). However, their expression declined at 35 and 45 min most likely due to a higher contribution to cell death from necrosis rather than apoptosis at the longer ischemic times (Fig. 20).

I then characterized expression of CtsD in IRI. Both forms of CtsD, pro- and mature one, followed similar expression pattern as active caspase-3 and cleaved PARP-1 with maximum expression at 25 min ischemia and a later decline in expression by 35 and 45 min ischemia (Fig. 20). GAPDH protein expression was unchanged and used as the WB loading control. Thus, and in agreement with the findings of the FA induced nephrotoxic model, CtsD was also up-regulated in AKI after ischemia reperfusion.

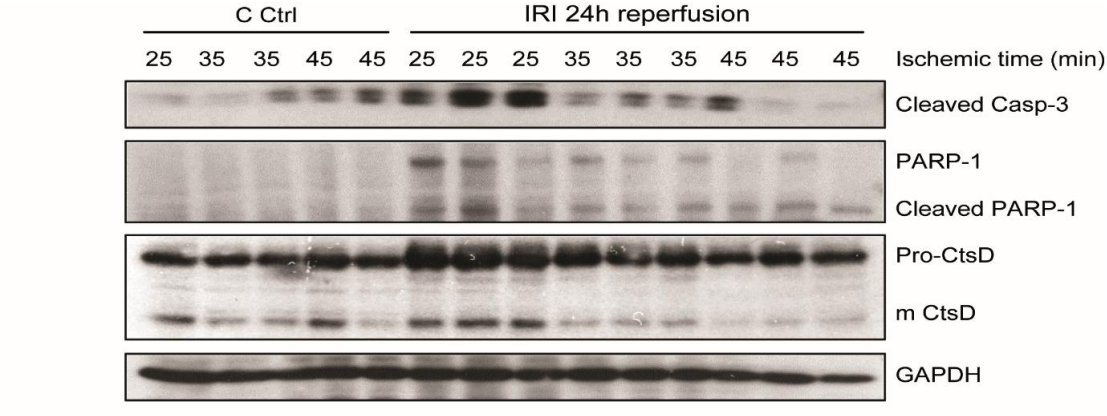

Figure 20: Western Blot of cleaved or active caspase-3, PARP-1 and cleaved PARP-1, pro- and mature CtsD and GAPDH in kidney lysates during increasing ischemic times (25, 35 and 45 min) and 24 h reperfusion in contralateral and IRI kidneys lysates.

In addition, CtsD expression was confirmed by CtsD immunostaining in control and 25 min IRI in paraffin embedded kidney tissues. As shown in figure 21 at the corticomedullary junction (CMJ) (A) or the cortex (B) of contralateral control kidney very little CtsD staining was detected and this was limited to a fine punctate pattern in some tubular cells (Fig. 21A-B).

However, in the left kidney after 25 min of the ischemic insult CtsD staining was stronger in epithelial tubular cells from the corticomedullary junction and the cortex (Fig. 21A-B). Interestingly, CtsD was predominately detected in damaged tubules characterised by tubular dilation and the presence of granular casts. Therefore, CtsD expression correlates with apoptosis in damaged epithelial tubular cells during IRI.

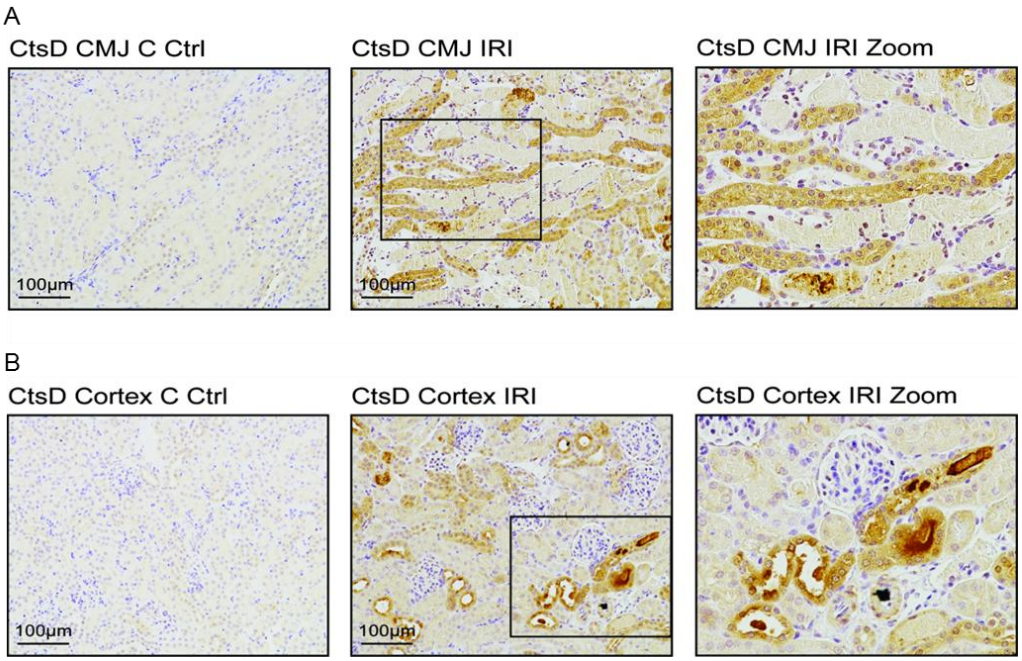

Figure 21: Representative pictures of CtsD immunostaining (brown) of CMJ **(A)** or cortex **(B)** from contralateral control kidneys and and 25 min ischemic 24 h reperfused kidneys.

5.4. Effect of CtsD pharmacological inhibition by Pepstatin A in IRI induced AKI model

CtsD is known to play a pro-apoptotic role in different cell types [54], however its role in IRI induced AKI is still unknown. The occurrence of IRI induced AKI can be predicted in some cases as occurs during renal transplant [59] or major surgery [60]. In those cases, pre-treatment before the ischaemic episode has potential therapeutic application. In order to simulate this scenario, I pre-treated the mice with CtsD inhibitor (Pepstatin A) 1 h before ischemia and again 4 h post-ischemia. I performed 25 min ischemia and 24 h reperfusion, conditions where both apoptosis and CtsD protein levels were highest in this model. Firstly, I analysed the activity of CtsD in kidney using a specific fluorescently label substrate. In agreement with Fig. 20, CtsD activity was significantly increased at 25 min after IRI in comparison with sham kidneys (Fig. 22). Pepstatin A reduced CtsD activity not only in IRI kidneys but also in sham operated kidneys.

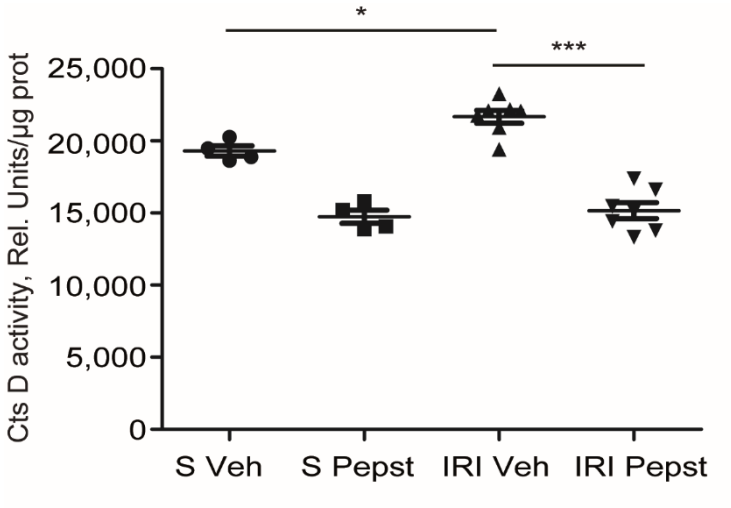

Figure 22: CtsD fluorometric activity in kidney lysates of sham and IRI vehicle or Pepstatin A treated animals. Ischemia was performed for 25 min and kidneys were reperfused for 24 h. Animals were treated with vehicle or Pepstatin A 20mg/Kg 1 h before surgery and 4 h post-surgery. Repeated measures t-test,*P ≤ 0.05 or ***P ≤ 0.001.

5.4.1. Effect of Pepstatin A on tubular cell damage during IRI induced AKI

Tubular injury was assessed in this animal model in the corticomedullary junction (CMJ), as it is the most affected area during IRI [5761]. The CMJ is highly susceptible to the damage induced by ischemia because of its low glycolytic capacity to produce ATP.

This compromises survival of cells located in the CMJ under ischaemic conditions. Tubular damage was assessed according to previously described AKI pathological scoring system [21] using the following criteria: tubular dilation and granular cast formation.

Pepstatin A significantly reduced the percentage of damaged tubules and the histomorphological injury score in the CMJ in IRI kidneys (Fig. 23A-B). Figure 23C shows representative PAS pictures of sham and IRI vehicle or Pepstatin A treated kidneys. From this data it is evident that CtsD inhibition by Pepstatin A reduces tubular cell damage after acute IRI.

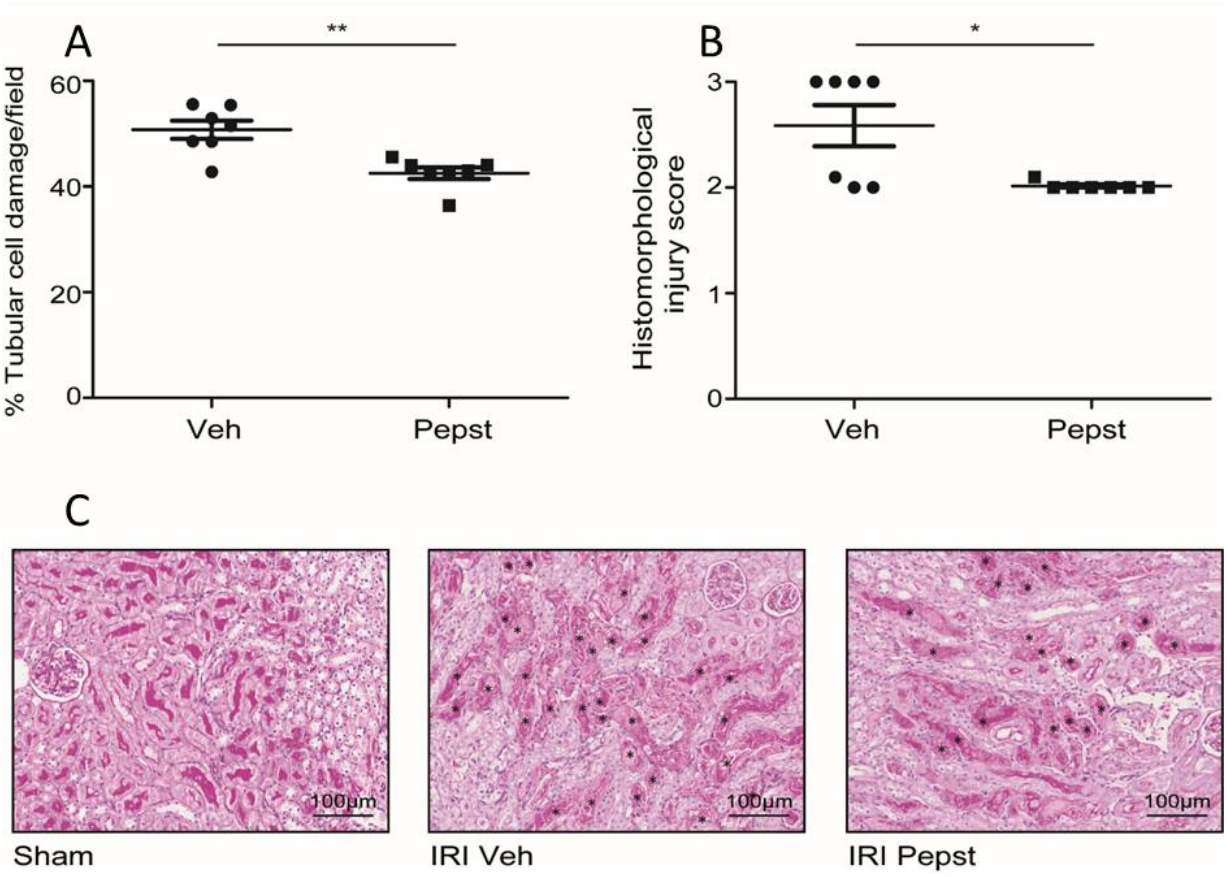

Figure 23: Percentage of tubular injury as assessed by tubular dilatation and granular cast formation in CMJ **(A)** and histomorphological injury score **(B)** of IRI vehicle or Pepstatin A treated kidneys. Representative PAS pictures* **(C)** of sham or IRI vehicle or Pepstatin A treated kidneys (damage tubules *). Ischemia was performed for 25 min and kidneys were reperfused for 24 h. Animals were treated with vehicle or Pepstatin A 20mg/Kg 1 h before surgery and 4 h post-surgery. Repeated measures t-test,*P ≤ 0.05 or **P ≤ 0.01.

5.4.2. Effect of CtsD inhibition on kidney inflammation during IRI induced AKI

IRI injury is triggered by the inflammatory response produced during the reperfusion phase which is driven by neutrophils amongst other inflammatory cells. CtsD is known to drive apoptosis in neutrophils through activation of caspase-8 [62], therefore, CtsD inhibition could lead to a sustained inflammatory response. Thus, I analysed the effect of Pepstatin A administration on inflammation in this model. Pepstatin A had not effect in the number of neutrophils observed in the CMJ after IRI (Fig. 24).

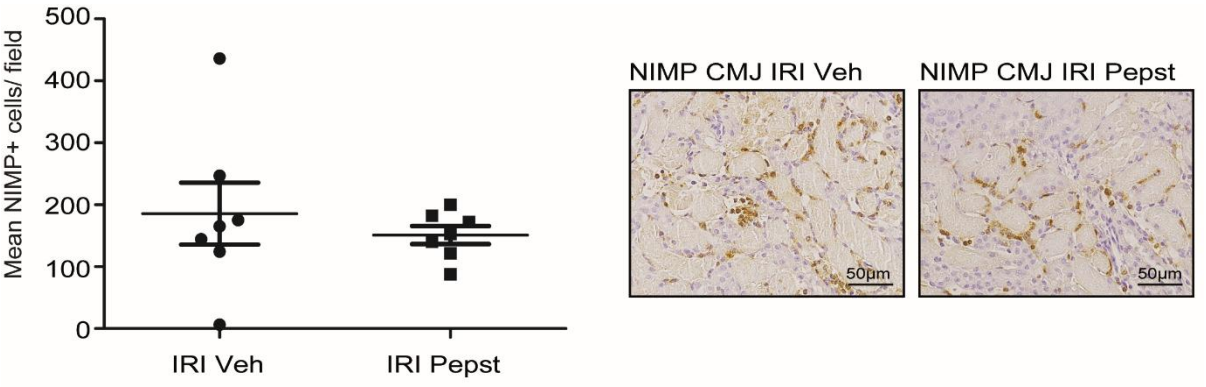

Figure 24: Average number of NIMP^{+} cells per field with representative pictures in the CMJ of IRI vehicle or Pepstatin A treated kidneys. Ischemia was performed for 25 min and kidneys were reperfused for 24 h. Animals were treated with vehicle or Pepstatin A 10mg/Kg 1 hr before surgery and 4 h post-surgery.

I then analysed the gene expression of AKI inflammatory mediators by RT-PCR. As in FA nephrotoxic injury model, I evaluated CXCL-1 and CXCL-2, IL-1β, IL-6, TNF-α and RANTES. The expression of inflammatory genes was increased in IRI but it was not significantly altered by Pepstatin A treatment (Fig. 25A-F). In summary, Pepstatin A did not have a major effect on inflammation during AKI.

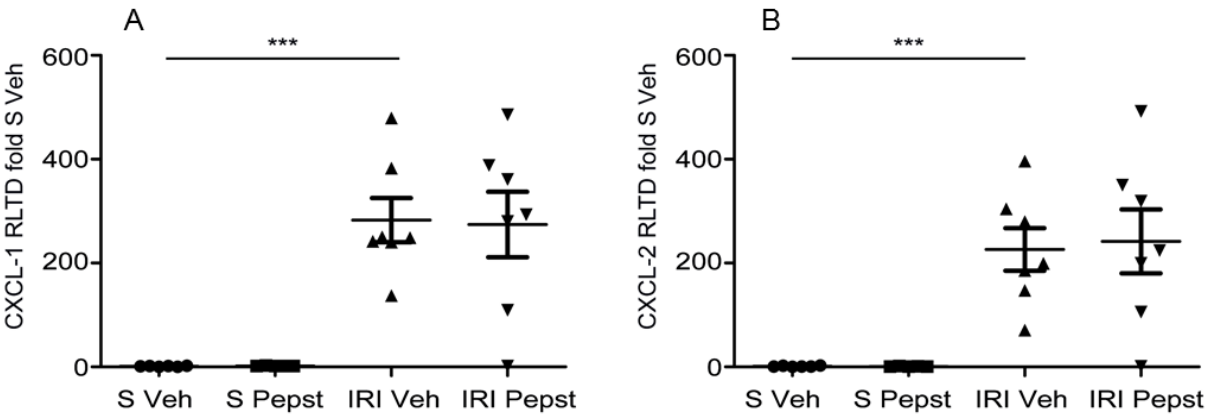

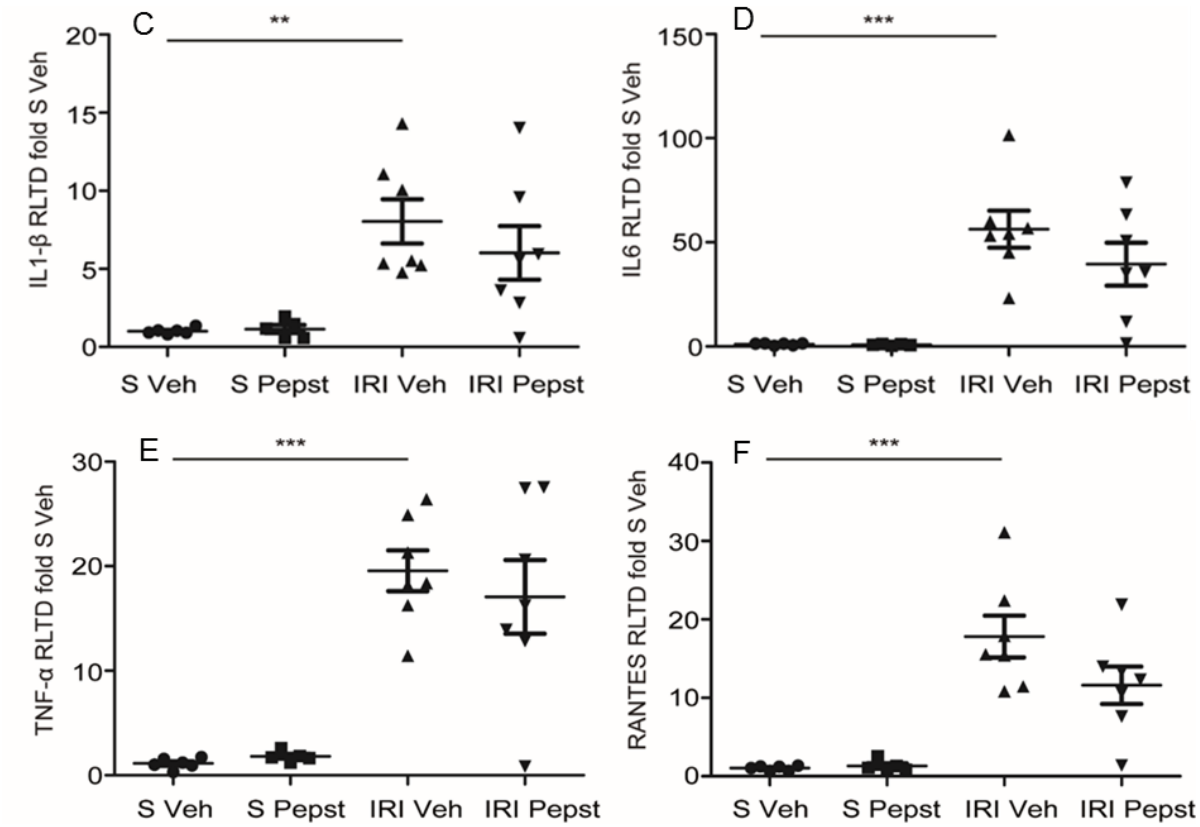

Figure 25: CXCL-1 **(A)**, CXCL-2 **(B)**, IL1-β **(C)**, IL-6 **(D)**, TNF-α **(E)** and RANTES **(F)** mRNA expression from sham and IRI vehicle or Pepstatin A treated kidneys. Ischemia was performed for 25 min and kidneys were reperfused for 24 h. Animals were treated with vehicle or Pepstatin A 20mg/Kg 1 h before surgery and 4 h post-surgery. Repeated measures t-test, **P ≤ 0.01, ***P ≤ 0.001.

5.4.3. Effect of Pepstatin A on apoptosis during IRI induced AKI

I next assessed the effect of Pepstatin A on apoptosis in IRI induced AKI. As shown in figure 26, an increase in cleaved or active caspase 3 in IRI kidneys was demonstrated by WB in comparison with contralateral control and sham kidneys. GAPDH protein expression was unchanged and used as the WB loading control. This increase was inhibited by Pepstatin A treatment. This data supporting my previous findings in the FA nephrotoxic model (Fig. 19A)

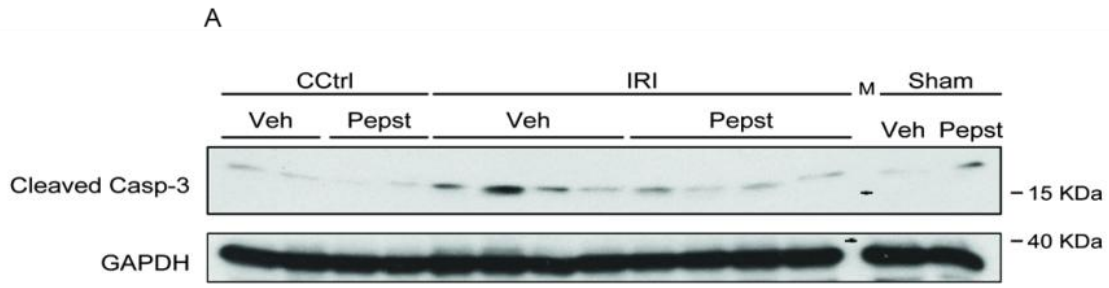

Figure 26: Cleaved caspase-3 and GAPDH WB of sham, control or IRI vehicle or Pepstatin A treated kidneys. Ischemia was performed for 25 min and kidneys were reperfused for 24 h. Animals were treated with vehicle or Pepstatin A 20mg/Kg 1 h before surgery and 4 h post-surgery.

In order to confirm Pepstatin A effect on apoptosis during IRI induced AKI TUNEL staining was performed. In agreement with the active caspase-3 WB, TUNEL staining confirmed a 40% reduction in the percentage of apoptotic cells ($TUNEL^{+}$) in the CMJ of IRI Pepstatin A treated animals compared to vehicle only treatment (Fig. 27).

No TUNEL positive cells were detected in the control kidneys. Thus, CtsD reduces tubular damage and apoptosis with no effect on the inflammatory response.

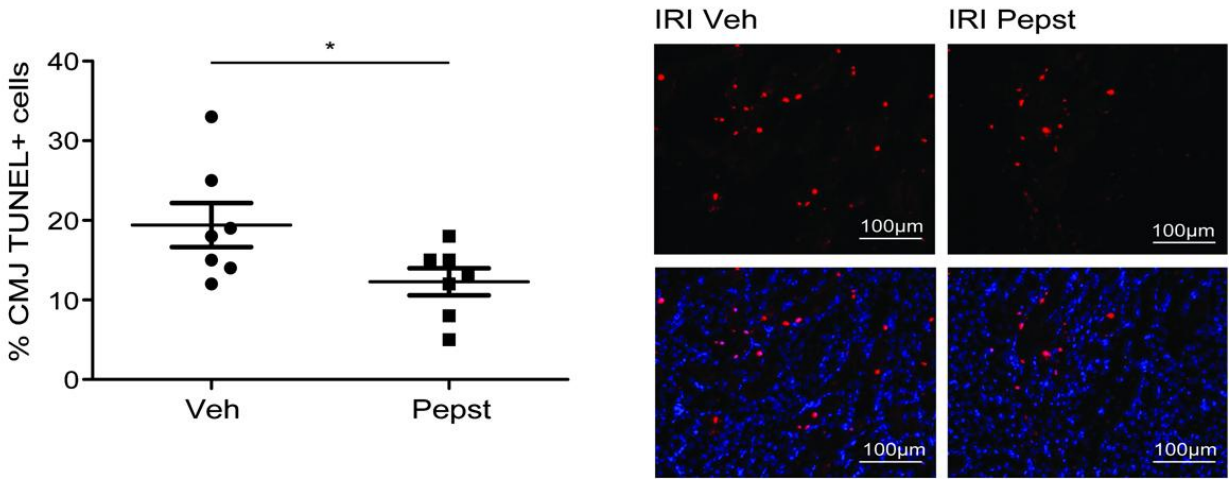

Figure 27: Percentage of cortical TUNEL positive cells versus total cells and representative TUNEL +/- DAPI pictures in IRI vehicle or Pepstatin A treated kidneys. Ischemia was performed for 25 minutes and kidneys were reperfused for 24 hour. Animals were treated with vehicle or Pepstatin A 20mg/Kg 1 hour before surgery and 4 hours post-surgery. Repeated measures t-test, *P ≤ 0.05.

5.5. Effect of CtsD inhibition on hypoxic induced in tubular epithelial cells

During IRI, tubular epithelial cells undergo hypoxia due to a decreased oxygen supply [63]. HKC-8 cells were seeded in six well plates and incubated in hypoxic and normoxic conditions.

Hypoxia-Inducible Factor (HIF)-1α is a hetero-dimeric transcription factor that plays an integral role in the body's response to low oxygen concentrations. HIF-1α is translocated into the nuclei hypoxic conditions where acts as master transcriptional regulator.

HIF-1α immunostaining in HKC-8 cells was performed after 48 h normoxic or hypoxic cultured conditions to confirm hypoxia (Fig.28). As expected hypoxia led to the translocation of HIF-1α from the cytosol, where is located in normoxic conditions (20% O_2), into the nuclei under low oxygen concentration (1% O_2).

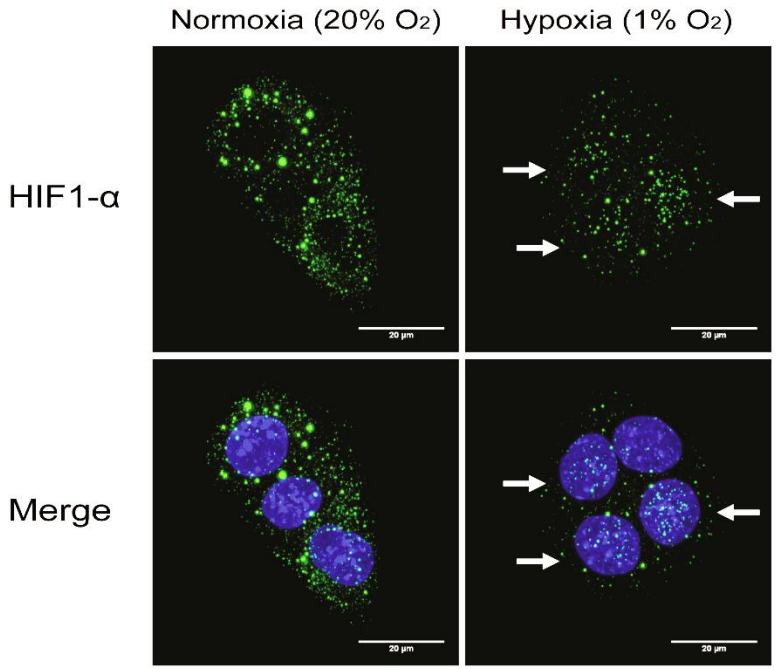

Figure 28: HIF-1α immunostaining in HKC-8 cells under normoxic (20% O_2/5% CO_2) or hypoxic (1% O_2/5% CO_2) cultured conditions for 48 h. The white arrows point to HIF-1α located within the nuclei.

Then, I assessed the effect of Pepstatin A on the cell viability using the MTT assay. HKC-8 cells were seeded in 24-well plates and left to attach overnight. The following morning they were treated with Pepstatin A 10µg/mL or vehicle (DMSO) for 48 h at 37°C in 20% or 1% O_2 concentration. The cells incubated in low concentration of O_2 showed significantly reduced the number of viable cells as expressed by the number of metabolically active cells in comparison with cells cultured in normal O_2 concentration (Fig. 29). Pepstatin A treatment significantly increased cell number under hypoxic conditions and had no effect under normoxic conditions.

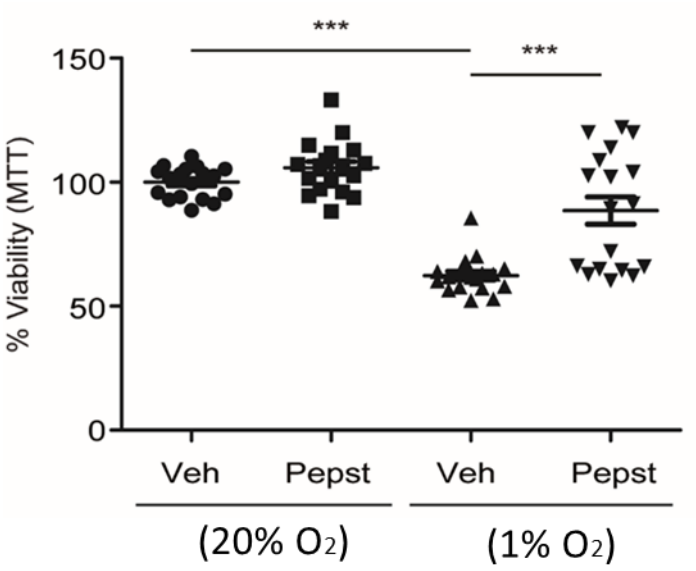

Figure 29: Percentage of metabolically active viable cells assessed by MTT assay in HKC-8 cells treated with vehicle or Pepstatin A (10µg/mL) under normoxic (20% O_2/5% CO_2) or hypoxic (1% O_2/5% CO_2) conditions for 48 h. Repeated measures t-test, ***P ≤ 0.001.

A reduction in cell number could be due to an increase in apoptosis induced by hypoxic conditions. In order to confirme this cleaved or active caspase-3, WB was performed in HKC-8 incubated for 48 h with Pepstatin A 10µg/mL or vehicle (DMSO) at 37°C in 1% O_2 concentration. Caspase-3 was decreased in hypoxic cells treated with Pepstatin A in comparison with cells treated with vehicle only (Fig.30). GAPDH protein expression was unchanged and used as the WB loading control.Thus *in vitro* result supports the *in vivo* IRI findings.

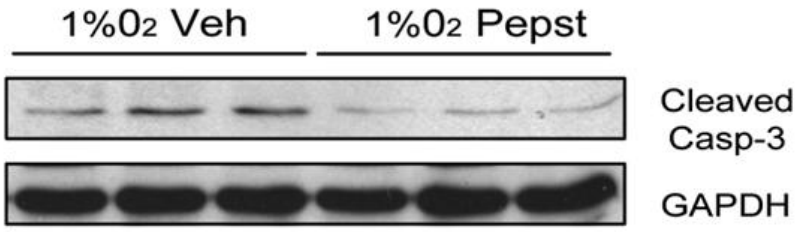

Figure 30: Cleaved or active caspase-3 and GAPDH WB in HKC-8 cells under hypoxic conditions for 48 h treated with vehicle or Pepstatin A (10µg/mL).

5.6. Effect of CtsD inhibition in a progressive model of renal fibrosis following IRI induced AKI

AKI predisposes to the development and exacerbation of chronic kidney disease (CKD) [59]. During AKI a normal repair response will restore the normal tubular epithelium. This process involves cell death, proliferation of normal viable tubular cells and reestablishment of cell polarity. However, an abnormal repair response (incomplete tubular repair, persistent inflammation, fibroblasts proliferation and excessive extracellular matrix deposition) will instead lead to CKD [7]. To analyse whether CtsD inhibition could have an effect on CKD induced by AKI, I performed an ischemia reperfusion injury chronic model.

In 8-10 week C57BL/6 females, the left renal pedicle was clamped for 35 min. Then, the clamp was removed and the kidney reperfused for 28 days. Sham animals underwent a mock surgical procedure. Vehicle or Pepstatin A (20mg/Kg) was administered by i.p. injection 1 h before surgery and from day 2 post-surgery three times a week up to 28 days. After 28 days, the animals were culled and blood, urine and kidneys were collected.

First of all, I analysed CtsD activity in kidney tissue using a specific fluorescently labelled substrate. IRI kidneys showed a significant increase in CtsD activity in compared with sham which was significantly reduced by pepstatin A treatment (Fig. 31).

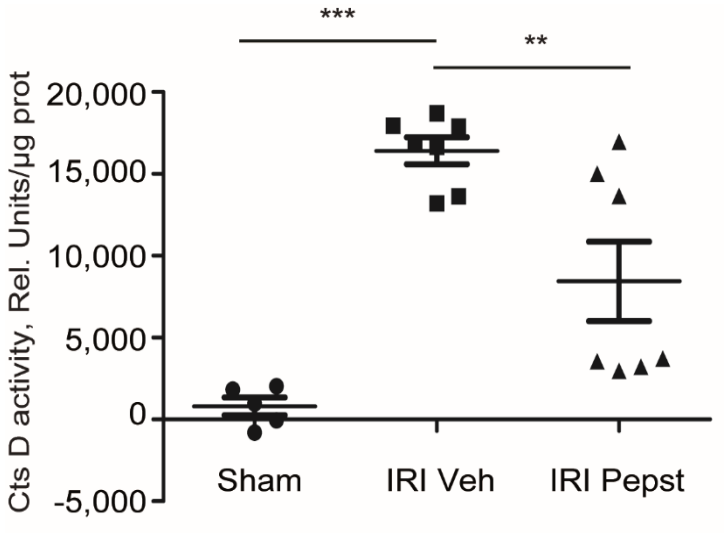

Figure 31: CtsD fluorometric activity in kidney lysates assessed by the cleavage of a specific fluorescently labelled substrate. Ischemia was performed for 35 minutes and kidneys were reperfused for 28 days. Animals were treated with vehicle or Pepstatin A 20mg/Kg 1 h before surgery and from day 2 post-surgery three times a week up to 28 days., Repeated measures t-test,. **P ≤ 0.01,***P ≤ 0.001.

5.6.1. Effect of Pepstatin A on apoptosis in a progressive model of renal fibrosis induced by IRI AKI

Next, cleaved or active caspase-3 WB was performed to analyse the effect of Pepstatin A on apoptosis in this chronic model (Fig.32). Cleaved caspase-3 WB confirmed an increase in apoptosis in IRI kidneys in comparison with sham kidneys and a decrease in IRI Pepstatin A treated kidneys.

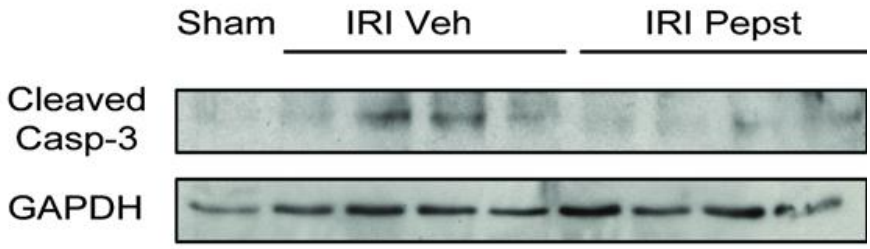

Figure 32: Cleaved caspase-3 and GAPDH WB in sham and IRI vehicle or Pepstatin A treated animals. Ischemia was performed for 35 min and kidneys were reperfused for 28 days. Animals were treated with vehicle or Pepstatin A 20mg/Kg 1 hour before surgery and from day 2 post-surgery three times a week up to 28 days.

5.6.2. Effect of Pepstatin A on interstitial fibrosis in a progressive model of renal fibrosis induced by IRI AKI

To determine whether apoptosis reduction led to an improvement of CKD progression, interstitial fibrosis was analysed. Ischemia was performed for 35 min and kidneys were reperfused for 28 days. Interstitial collagen, as assessed by Sirius Red staining, was significantly reduced by Pepstatin A treatment in IRI kidneys compared with IRI vehicle (Fig. 33A).

However, Pepstatin A did not have any effect on the number of interstitial myofibroblasts (Fig. 33B). Furthermore, collagen synthesis was analysed by collagen 1A1 and collagen 3A1 gene expression. Gene expression for collagen 1A1 and collagen 3A1 was significantly decreased in IRI Pepstatin A treated kidneys (Fig.33C-D). Therefore, early treatment with Pepstatin A slowed fibrosis development as a consequence of ischemic AKI.

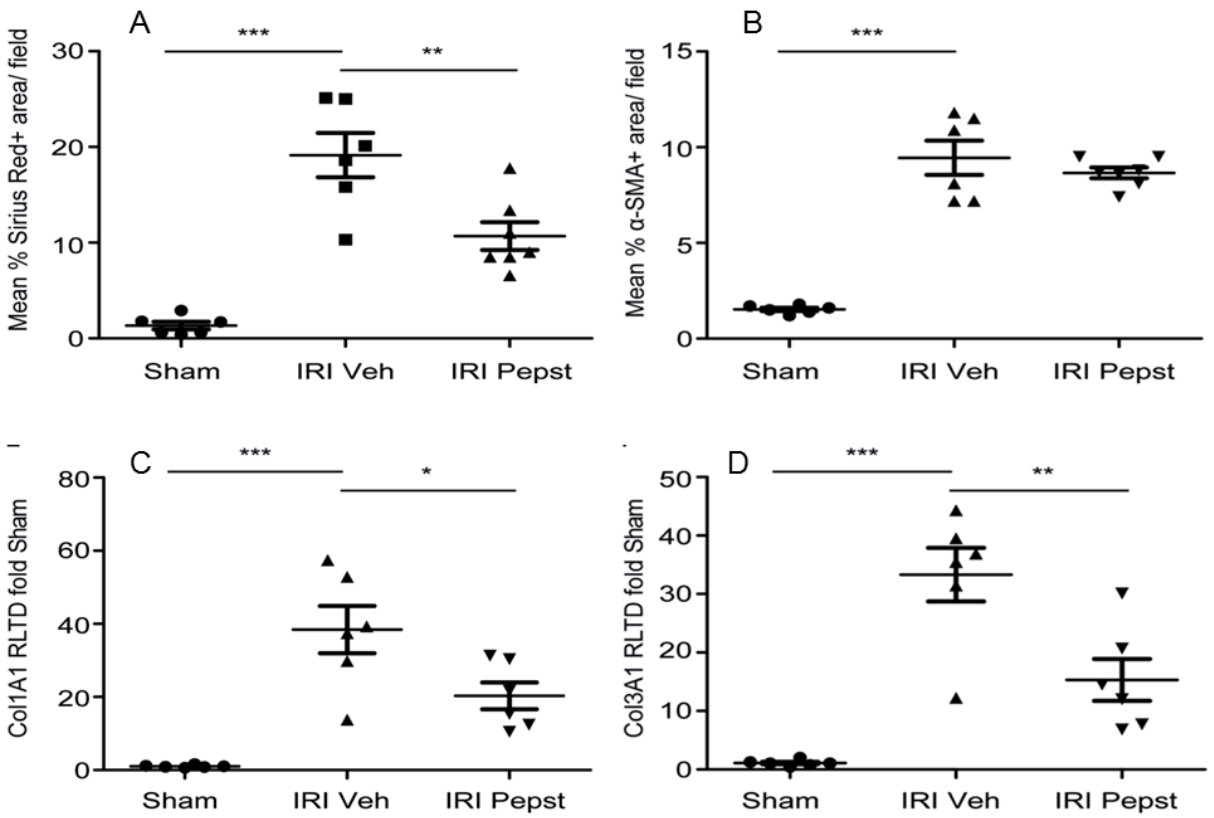

Figure 33: Morphometric analysis of interstitial collagen (SR+ area/field) **(A)** or interstitial myofibroblast (α-SMA+ area/field) **(B)** of kidney cortex from sham and IRI vehicle or Pepstatin A treated kidneys. Col1A1 **(C)** and Col3A1 **(D)** kidney mRNA expression from sham and IRI vehicle or Pepstatin A treated kidneys. Ischemia was performed for 35 min and kidneys were reperfused for 28 days. Animals were treated with vehicle or Pepstatin A 20mg/Kg 1 hour before surgery and from day 2 post-surgery three times a week up to 28 days. Repeated measures t-test, *P ≤ 0.05, **P ≤ 0.01,***P ≤ 0.001.

5.7. CtsD expression in acute tubular necrosis transplant kidney human biopsies

The results obtained demonstrate that CtsD inhibition by Pepstatin A represents a good therapeutic approach to reduce apoptosis, tubular damage and improve kidney function in mouse AKI. Pepstatin A administration also improved CKD progression from ischemic AKI, reducing apoptosis and interstitial fibrosis. In order to validate some of my findings in human disease, CtsD immunostaining was

performed in acute tubular necrosis (ATN) transplanted patient biopsies. CtsD was highly expressed in tubular epithelial cells in these patients (Fig. 34) compared to previous reports in normal human kidney [64]. Moreover, CtsD expression appeared to correlate with the degree of tubular damage. Thus, injured tubules characterised by loss of brush border, granular cast formation, tubular dilatation and epithelial cell vacuolisation had higher CtsD expression than less damaged cells.

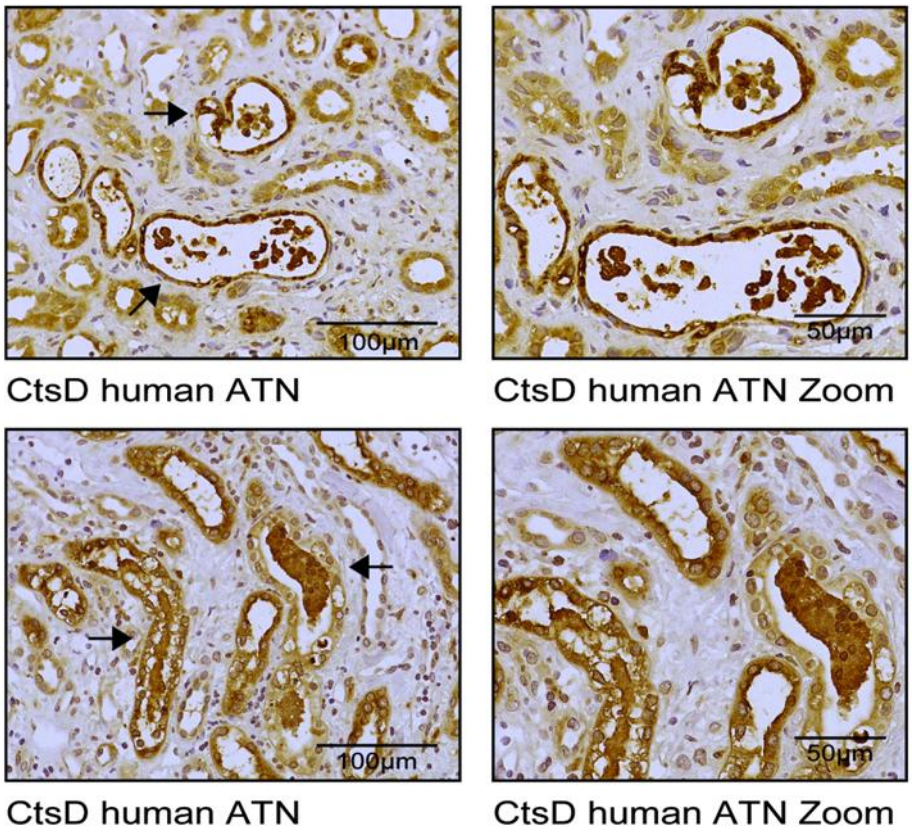

Figure 34: Representative pictures of CtsD immunostaining (brown) in ATN transplanted human kidney biopsies. Black arrows point at damaged tubular cells with granular casts.

During apoptosis CtsD is released from the lysosomes into the cytosol due to lysosomal membrane permeabilisation (LMP), where it can play an active role in the apoptotic pathway [54]. To further study CtsD expression during cell death in ATN patients, CtsD (green) was co-stained with TUNEL (red) in these transplant biopsies.

During ATN, CtsD was expressed in non-apoptotic ($TUNEL^-$) and apoptotic ($TUNEL^+$) epithelial tubular cells (Fig. 35A). However, its cellular distribution changed depending on whether cells were undergoing apoptosis. While CtsD was distributed within vacuoles, most likely lysosomes, in non-apoptotic tubular epithelial cells (Fig. 35B), in apoptotic cells CtsD was evident in the cytosol (Fig. 35C). This observation suggests translocation of CtsD from the lysosome into the cytosol during apoptosis in human ATN. My findings support a possible role for CtsD during tubular epithelial cell death in transplant kidneys with ATN.

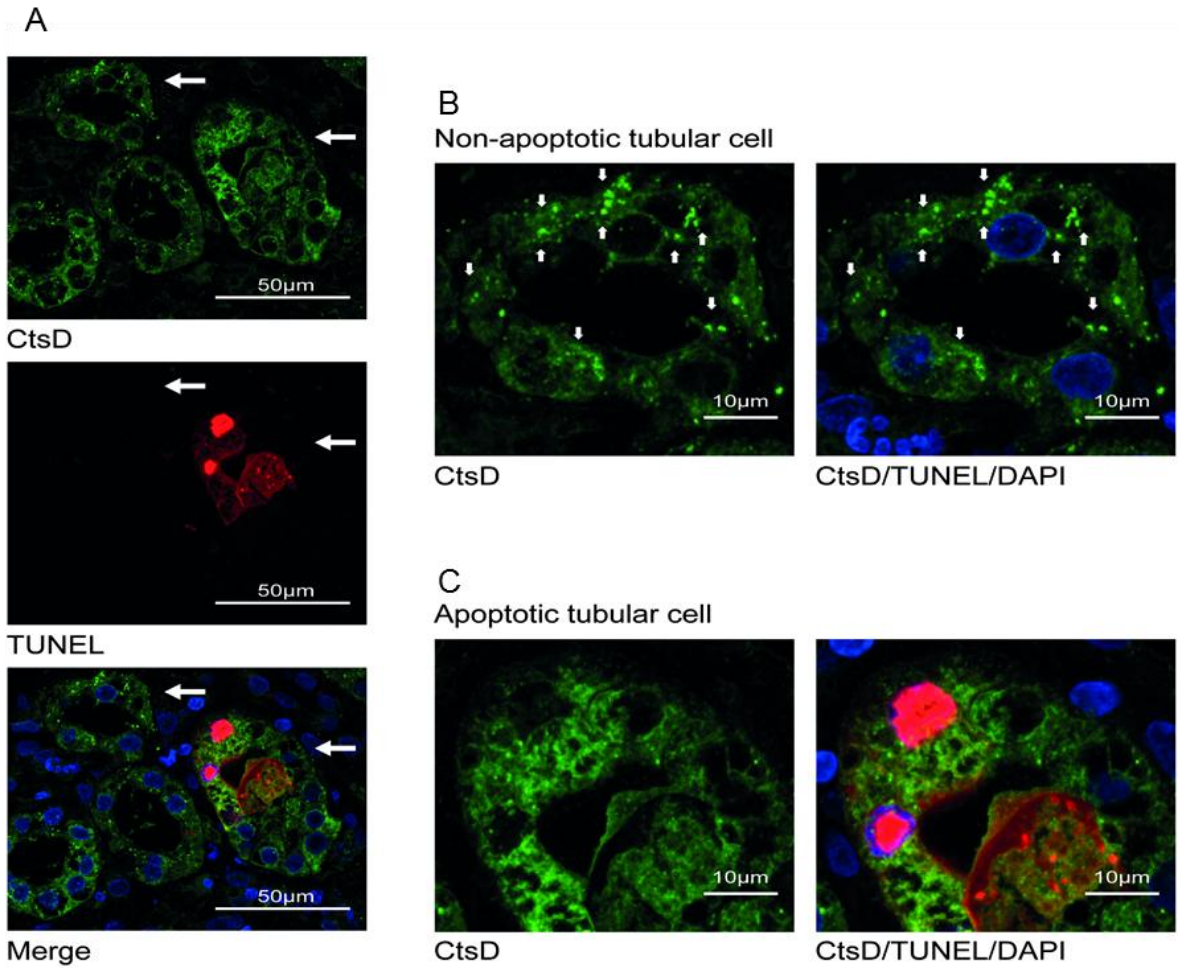

Figure 35: CtsD (green)/TUNEL (red) dual immunostaining in ATN transplanted human kidney biopsy. White arrows point to non-apoptotic and apoptotic tubular cells **(A)**. Detail CtsD distribution in a non-apoptotic tubular epithelial cell (TUNEL-/CtsD+) **(B)**. Detail CtsD distribution in an apoptotic tubular epithelial cell (TUNEL+/CtsD+) **(C)**.

6 DISCUSSION

Acute kidney injury (AKI) incidence has risen over the last decades due to the aging population and the comorbidities associated with these patients [65]. It is a common complication in hospitalised patients. The association between the development of AKI and higher in-hospital mortality has been well known for decades and reported in several studies [66]. As a conservative estimate, in the U.S. about 17 million admissions a year are complicated by AKI, resulting in additional costs to the health care system of $10 billion [8]. AKI is often under-recognised and associated with elevated risk of long-term adverse outcomes in hospitalised patients[67].

It is also a frequent and serious complication encountered in 30% to 50% of subjects after cardiopulmonary bypass (CPB) [68]. AKI requiring dialysis in CPB patients occurs in up to 5%, in whom the mortality rate approaches 80%, and is the strongest independent risk factor for death after CPB. AKI also contributes to delayed graft function (DGF after transplantation) as ischemia reperfusion induced AKI occurs in 20-80% of deceased donor kidneys, with detrimental effects for both graft life and patient survival.

Finally, maladaptive repair following AKI contributes to the development or exacerbation of chronic kidney disease (CKD) and end-stage renal disease (ESRD) [34]. Despite the progress in the management of AKI, its mortality rate over the last 50 years remains unchanged at around 50% [69]. Therefore, there is an urgent need for specific therapies against AKI. Thus, better knowledge about the cellular mechanisms driving AKI is crucial in order to find new therapeutic candidates.

AKI is a complex disease which can be caused by a variety of insults, however, all of them lead to epithelial tubular cell death and loss of kidney function.

When apoptosis is deregulated, cells either fail to die, as in a number of pathologies such as cancer and other hyperproliferative diseases, or die excessively, as in a number of neurodegenerative disorders [70]. Proteases play a central role in the execution phase of apoptosis, and the caspases, a family of cysteine proteases, are of major importance.

A number of other proteases, including granzymes, cathepsins and calpains, have been also found to be involved in cell death [71]. The basic function of a protease is to irreversibly modulate the properties of other proteins by cleaving them. As a consequence of a cleavage or a series of cleavages, proteins either gain a function, activation by limited proteolysis or lose a function, ultimately being turned over. Proteases are generally synthesised as inactive precursors that require activation, most often by limited proteolysis, thereby being protease substrate themselves. Due to this irreversibility, protease signalling is an effective way of killing a cell, as the cell death, once the program has started, cannot be reversed or prevented.

Apoptosis signal transduction pathways have been found to occur in the cytoplasm, on the inner surface of the plasma membrane, in mitochondria, and in the nucleus. In particular, caspase-mediated signalling occurs predominantly in the cytoplasm. In contrast, cathepsins are localised in lysosomes, or are secreted by the cell. This raises the question as to how these enzymes can facilitate apoptosis signalling. An emerging line of evidence suggests that during apoptosis, cathepsins are translocated from lysosomes to other subcellular locations.

It remains unclear, however, whether this is a general apoptosis phenomenon, or it is restricted to execution induced by only some apoptotic stimuli. In addition, it is unclear whether the release of cathepsins from lysosomes is controlled by pores or translocators, or it is simply the consequence of damage to

lysosomal membranes during the apoptotic process. To date, relatively little is known about potential intersections of cathepsin and caspase-mediated pathways, although it seems likely that these pathways may be integrated in some fashion.

Lysosomal proteases such as CtsD can play multiple roles in apoptosis by degrading different substrates and/or contributing to mitochondrial destabilisation [72]. CtsD is a lysosomal proteinase that may constitute as much as 10% of the soluble lysosomal proteins and whose concentration in liver lysosomes can be as high as 0.7 mM. Being a major component of the lysosome, CtsD is found in nearly all mammalian cell types and tissues [73]. Very little is known about the role of CtsD in kidney disease. A recent report identified CtsD as a possible novel prognostic marker for AKI in a urinary proteomic analysis. In this study, two proteins, IGFBP-7 and CtsD, were validated by proteomics and ELISA as differentially regulated in urine from late/non-recovery versus early recovery AKI patients [74]. Despite this evidence indicating a possible role of CtsD in cell death during AKI, its contribution is still unknown.

My experiment work describes an increase of CtsD expression in two different models of AKI, nephrotoxic and ischemia induced (Fig. 15A, 20). CtsD was highly expressed in damaged tubular cells during both types of injury in comparison with sham or control kidneys, pointing towards a possible contribution of CtsD to cell death during AKI (Fig. 15B, 21).

In agreement with my findings in mouse AKI, CtsD analysis in human transplanted biopsies with ATN confirmed high levels of CtsD in damaged tubular epithelial cells. During apoptosis, lysosomal membrane permeabilisation allows translocation of CtsD from the lysosome into the cytosol, where it exerts its pro-apoptotic function. Indeed, microinjection of CtsD into the cytosol is sufficient to

trigger mitochondrial permeabilisation, cytochrome c release and apoptosis which is prevented by caspase-3 or CtsD inhibitor Pepstatin A [75].

When analysing CtsD cellular distribution in human ATN, CtsD location seemed to change being mainly cytosolic in cells undergoing apoptosis and contained within vesicles, most likely lysosomes, in non-apoptotic cells (Fig. 35). CtsD optimal activity occurs in the acidic pH found within lysosomes. Although CtsD is still active at cytosolic neutral pH, its half life is limited due to the reversible deprotonation of the active aspartate site [72]. However, there are several mechanisms that might contribute to prolong CtsD activity during apoptosis, such as cytosolic acidification [76] or substrate binding. *In vitro* studies have also shown that CtsD can display significant activity at a pH greater than 6.5 [77]. In addition, in cultured fibroblasts CtsD has also being reported as able to induce apoptosis at pH 7.0, therefore it is likely to be proteolytically active and cleaving substrates outside the lysosomal compartment [75]. I confirm CtsD activity in my studies showing a significant increase during AKI (Fig. 22, 31).

To further analyse the role of CtsD during cell death in AKI, I used the CtsD inhibitor, pepstatin A. Pepstatin A is the best available inhibitor against CtsD, however, it can affect at mach lower level other proteases of aspartic endopeptidase A1 family. Most of the proteases of the A1 family are specifically expressed in other organs, such as stomach (Pepsin and CtsE) or central nervous system (BACE-1 and -2). Although renin is expressed in kidney, Pepstatin A is a weak rennin inhibitor, to the extent that 26,000 times more Pepstatin A is needed to inhibit renin (Ki=13000 µmol/L) at the same level than CtsD (Ki=0.5 µmol/L) [78]. Therefore and despite I cannot exclude additional effects on other A1 peptidases in my studies, it is unlikely that they would be the main contributors.

CtsD knock-out mice develop massive neuronal cell death and die approximately 26 days after birth due to neurological disorders [79], replicating human deficiency [8081].

Pepstatin A dose for my studies was more than 50 times below the previously described IC50 [82]; at this dose Pepstatin A reduced CtsD activity without complete inhibition (Fig. 22, 31), which could have led to possible undesirable secondary and systemic effects. I first analysed the effect of CtsD inhibition on inflammation as cathepsins play an important role in the immune response [58] modulating tissue damage and cell death. Specifically, CtsD plays an important role driving neutrophil apoptosis by directly activating the initiator caspase-8. CtsD deficiency leads to delayed neutrophil apoptosis and amplified and a prolonged innate immune response [83]. CtsD inhibition did not induce any changes in neutrophil infiltration (Fig. 24).

Gene expression analysis of common inflammatory mediators of AKI was also not altered by Pepstatin A treatment (Fig. 18, 24). Administration of Pepstatin A significantly improved kidney function (Fig. 16) in the nephrotoxic induced AKI model and reduced apoptotic tubular cell death in both models (Fig. 19,26,27), showing an overall reduction in the number of damaged tubular cells (Fig. 17, 23). Pepstatin A effect on apoptosis was confirmed in human tubular epithelial cells under hypoxic conditions (1% O_2) (Fig. 29,30). It is therefore possible that Pepstatin A reduces functional and histological tubular injury by reducing apoptotic cell death. Proving a causal link between reduced apoptosis and favourable renal outcomes is difficult *in vivo*, but the cell protective effects of Pepstatin A are supported by the *in vitro* data presented.

In my studies, I have not pursued further the mechanism of action behind CtsD during apoptosis in AKI. However, according to previous literature it is likely

that CtsD might be involved in either inactivating antiapoptotic proteins or activating proapoptotic factors. In that respect, it is known that LMP followed by release of cathepsins into the cytosol initiates apoptotic signalling, often via the intrinsic apoptotic pathway [84]. This pathway is characterized by mitochondrial outer membrane permeabilisation (MOMP) and release of apoptogenic factors, including Cytochrome c into the cytosol.

Mitochondrial membrane integrity is regulated by the BCL-2 protein family, which consists of both antiapoptotic and proapoptotic members, the latter of which includes BAX and BID [85]. Under normal conditions, BAX is located in the cytosol in an inactive form, but upon induction of apoptosis, BAX translocates to the mitochondria where it triggers MOMP. Bid, which generally requires proteolytic processing to become proapoptotic, induces conformational changes in BAX, leading to its activation and oligomerisation, which favours MOMP. Bid can be cleaved by a number of proteases, including caspase-8, granzyme B, calpains, and cysteine cathepsins. In addition to BID, antiapoptotic BCL-2 proteins and XIAP have been shown to be cleaved by cysteine cathepsins during apoptosis. Less is known about the targets of the aspartic protease CtsD after its release into the cytosol. Bid has been suggested to be a target of CtsD, but the reports are not conclusive [86]

AKI can contribute or exacerbate the progression of CKD due to an abnormal or incomplete repair response. I have previously shown that Pepstatin A treatment from day 5 after IRI results in reduction of renal fibrosis due to an increase in collagen degradation with no effect on collagen gene transcription. In aur previous study a novel mechanism was proposed by which CtsD inhibition by Pepstatin A leads to an increase in extracellular protease activity, in particular UPA, due to altered lysosomal recycling. This could trigger a proteolytic cascade activating first

plasminogen into plasmin and culminating with the regulation and activation of MMPs. Both plasmin37–39 and MMPs are able to degrade extracellular matrix proteins causing a net reduction in fibrosis. This situation can be further sustained by a positive feedback loop, as plasmin is also able to activate UPA [87]. In this thesis Pepstatin A pre-treatment before IRI seems to have additional beneficial effect over the development of the injury. As well as a decrease in interstitial collagen (Fig. 33), I have also observed a decrease in apoptosis (Fig. 32) and a reduction in the expression of pro-fibrotic genes (Fig. 33). I propose that CtsD can influence disease progression by a dual mechanism of action contributing to apoptosis in the acute phase and to collagen turnover during the chronic phase. The protection from both acute injury and subsequent progression to CKD identifies CtsD, and potentially other proteases, as potential therapeutic targets.

In summary, in this thesis I report CtsD as an important mediator for apoptotic cell death during AKI. My work has focused on the role of CtsD, however, I cannot discard the participation of other lysosomal proteases such as CtsB or L during AKI, so further investigation will need to be done to clarify this. New therapies to reduce apoptotic cell death during AKI are already under study (caspase inhibitors, p53 inhibitors and PARP inhibitors). Pepstatin A have been safely used in clinical trials for duodenal ulcer as well as HIV experimental studies [88], however, it has problems such as poor solubility and low bioavailability.

New molecules to inhibit CtsD have been designed in recent years, opening new possibilities for better targeting of CtsD. In order to improve bioavailability and improve *in vivo* half-life, recent research has focused on smaller inhibitors that contain non-peptide functionalities in place of the peptide bond cleavage site of the

substrate. My work opens new and exciting prospect for the treatment of AKI by inhibiting lysosomal protease induced apoptosis.

7. CONCLUSIONS

The data from this thesis has demonstrated the important role of CtsD in AKI. In fact, CtsD expression is upregulated in two murine models of nephrotoxic and ischemic induced AKI. CtsD was highly expressed in kidney damaged tubular epithelial cells during both types of injury in comparison with sham or control kidneys, pointing towards a possible contribution of CtsD to cell death during AKI. CtsD role during the AKI was analysed by using its inhibitor Pepstatin A. CtsD inhibition did not induce in our models any changes in neutrophil infiltration. Gene expression analysis of common inflammatory mediators of AKI was also not altered by Pepstatin A treatment. Therefore CtsD inhibition did not have a major effect on inflammation during AKI.

Administration of Pepstatin A significantly improved kidney function in the folic acid nephrotoxic induced AKI model and reduced apoptotic tubular cell death in both models, showing an overall reduction in the number of damaged tubular cells. Pepstatin A effect on apoptosis was confirmed in human tubular epithelial cells under hypoxic conditions (1%O_2).

It is therefore possible that Pepstatin A reduces functional and histological tubular injury by reducing apoptotic cell death. AKI can contribute or exacerbate the progression of CKD due to an abnormal or incomplete repair response. Pepstatin A pre-treatment before IRI had additional beneficial effect over the progression of the injury towards renal fibrosis. In addition to a decrease in interstitial collagen, we also observed a decrease in apoptosis and a reduction in the expression of pro-fibrotic genes.

In agreement with our findings in mouse AKI, CtsD analysis in human transplanted biopsies with ATN confirmed high levels of CtsD in damaged tubular epithelial cells.

In summary, in this thesis I report for the first time CtsD as an important mediator for apoptotic cell death during AKI and its inhibition as a possible novel treatment for AKI. My thesis opens new and exciting avenues for the treatment of AKI by inhibiting lysosomal protease induced apoptosis.

8. REFERENCES

1. Glodny, B. *et al.* Normal kidney size and its influencing factors - a 64-slice MDCT study of 1.040 asymptomatic patients. *BMC Urol.* **9,** 19 (2009).

2. Bonventre, J. V. & Yang, L. Cellular pathophysiology of ischemic acute kidney injury. *J. Clin. Invest.* **121,** 4210–4221 (2011).

3. Madsen, K. M. & Tisher, C. C. Structural-functional relationships along the distal nephron. *Am. J. Physiol.* **250,** F1–15 (1986).

4. Kapitsinou, P. P. & Haase, V. H. Molecular Mechanisms of Ischemic Preconditioning in the Kidney. *Am. J. Physiol. - Ren. Physiol.* ajprenal.00224.2015 (2015). doi:10.1152/ajprenal.00224.2015

5. Jo, S. K., Rosner, M. H. & Okusa, M. D. Pharmacologic treatment of acute kidney injury: why drugs haven't worked and what is on the horizon. *Clin. J. Am. Soc. Nephrol.* **2,** 356–65 (2007).

6. Mehta, R. L. *et al.* Acute Kidney Injury Network: report of an initiative to improve outcomes in acute kidney injury. *Crit. Care* **11,** R31 (2007).

7. Coca, S. G., Yusuf, B., Shlipak, M. G., Garg, A. X. & Parikh, C. R. Long-term Risk of Mortality and Other Adverse Outcomes After Acute Kidney Injury: A Systematic Review and Meta-analysis. *Am. J. Kidney Dis.* **53,** 961–973 (2009).

8. Chertow, G. M., Burdick, E., Honour, M., Bonventre, J. V & Bates, D. W. Acute kidney injury, mortality, length of stay, and costs in hospitalized patients. *J. Am. Soc. Nephrol.* **16,** 3365–70 (2005).

9. Wang, H. E., Muntner, P., Chertow, G. M. & Warnock, D. G. Acute Kidney Injury and Mortality in Hospitalized Patients. *Am. J. Nephrol.* **35,** 349–355 (2012).

10. White, L. E., Chaudhary, R., Moore, L. J., Moore, F. A. & Hassoun, H. T. Surgical Sepsis and Organ Crosstalk: The Role of the Kidney. *J. Surg. Res.* **167,** 306–315 (2011).

11. Grams, M. E. & Rabb, H. The distant organ effects of acute kidney injury. *Kidney Int.* **81,** 942–8 (2012).

12. Lyman, J. L. Blood urea nitrogen and creatinine. *Emerg. Med. Clin. North Am.* **4,** 223–33 (1986).

13. Bauer, J. H., Brooks, C. S. & Burch, R. N. Renal function studies in man with advanced renal insufficiency. *Am. J. Kidney Dis.* **2,** 30–5 (1982).

14. Levey, A. S., Perrone, R. D. & Madias, N. E. Serum creatinine and renal function. *Annu. Rev. Med.* **39,** 465–90 (1988).

15. Baghdadi, M., Takeuchi, S., Wada, H. & Seino, K.-I. Blocking monoclonal antibodies of TIM proteins as orchestrators of anti-tumor immune response. *MAbs* **6,** 1124–1132 (2014).

16. Bolignano, D. *et al.* Neutrophil Gelatinase–Associated Lipocalin (NGAL) as a Marker of Kidney Damage. *Am. J. Kidney Dis.* **52,** 595–605 (2008).

17. Westenfelder, C. Earlier diagnosis of acute kidney injury awaits effective therapy. *Kidney Int.* **79,** 1159–61 (2011).

18. Perico, N., Cattaneo, D., Sayegh, M. H. & Remuzzi, G. Delayed graft function in kidney transplantation. *Lancet (London, England)* **364,** 1814–27

19. Shoskes, D. Warming to non-heart-beating donors? *Am. J. Transplant* **1,** 305–6 (2001).

20. Cosio, F. G. *et al.* Impact of acute rejection and early allograft function on renal allograft survival. *Transplantation* **63,** 1611–5 (1997).

21. Basile, D. P., Anderson, M. D. & Sutton, T. A. in *Comprehensive Physiology* (John Wiley & Sons, Inc., 2012). doi:10.1002/cphy.c110041

22. González, E. *et al.* Early steroid treatment improves the recovery of renal function in patients with drug-induced acute interstitial nephritis. *Kidney Int.* **73,** 940–6 (2008).

23. Abdel-Kader, K. & Palevsky, P. M. Acute Kidney Injury in the Elderly. *Clin. Geriatr. Med.* **25,** 331–358 (2009).

24. Sakacı, T. *et al.* Clinical outcomes and mortality in elderly peritoneal dialysis patients. *Clinics* **70,** 363–368 (2015).

25. Munshi, R., Hsu, C. & Himmelfarb, J. Advances in understanding ischemic acute kidney injury. *BMC Med.* **9,** 11 (2011).

26. Shirali, A. & Pazhayattil, G. S. Drug-induced impairment of renal function. *Int. J. Nephrol. Renovasc. Dis.* 457 (2014). doi:10.2147/IJNRD.S39747

27. Perazella, M. A. Drug-induced nephropathy: an update. *Expert Opin. Drug Saf.* **4,** 689–706 (2005).

28. Kim, S.-Y. & Moon, A.-R. Drug-Induced Nephrotoxicity and Its Biomarkers. *Biomol. Ther.* **20,** 268–272 (2012).

29. Kapitsinou, P. P. & Haase, V. H. Molecular mechanisms of ischemic preconditioning in the kidney. *Am. J. Physiol. Renal Physiol.* **309,** F821–34 (2015).

30. Schrier, R. W., Wang, W., Poole, B. & Mitra, A. Acute renal failure: definitions, diagnosis, pathogenesis, and therapy. *J. Clin. Invest.* **114,** 5–14 (2004).

31. Massberg, S. & Messmer, K. The nature of ischemia/reperfusion injury. *Transplant. Proc.* **30,** 4217–23 (1998).

32. Kang, K. J. Mechanism of hepatic ischemia/reperfusion injury and protection against reperfusion injury. *Transplant. Proc.* **34,** 2659–61 (2002).

33. Devarajan, P., Mishra, J., Supavekin, S., Patterson, L. T. & Steven Potter, S. Gene expression in early ischemic renal injury: clues towards pathogenesis, biomarker discovery, and novel therapeutics. *Mol. Genet. Metab.* **80,** 365–76 (2003).

34. Venkatachalam, M. A., Weinberg, J. M., Kriz, W. & Bidani, A. K. Failed Tubule Recovery, AKI-CKD Transition, and Kidney Disease Progression. *J. Am. Soc. Nephrol.* **26,** 1765–76 (2015).

35. Kalimuthu, S. & Se-Kwon, K. Cell Survival and Apoptosis Signaling as Therapeutic Target for Cancer: Marine Bioactive Compounds. *Int. J. Mol. Sci.* **14,** 2334–2354 (2013).

36. Bröker, L. E., Kruyt, F. A. E. & Giaccone, G. Cell death independent of caspases: a review. *Clin. Cancer Res.* **11,** 3155–62 (2005).

37. Tait, S. W. G. & Green, D. R. Mitochondria and cell death: outer membrane permeabilization and beyond. *Nat. Rev. Mol. Cell Biol.* **11,** 621–32 (2010).

38. Edinger, A. L. & Thompson, C. B. Death by design: apoptosis, necrosis and autophagy. *Curr. Opin. Cell Biol.* **16,** 663–9 (2004).

39. Berghe, T. Vanden, Linkermann, A., Jouan-Lanhouet, S., Walczak, H. & Vandenabeele, P. Regulated necrosis: the expanding network of non-apoptotic cell death pathways. *Nat. Rev. Mol. Cell Biol.* **15,** 135–147 (2014).

40. Appelqvist, H., Wäster, P., Kågedal, K. & Öllinger, K. The lysosome: from waste bag to potential therapeutic target. *J. Mol. Cell Biol.* **5,** 214–26 (2013).

41. Turk, B. & Turk, V. Lysosomes as ‘suicide bags’ in cell death: myth or reality? *J. Biol. Chem.* **284,** 21783–7 (2009).

42. Boya, P. & Kroemer, G. Lysosomal membrane permeabilization in cell death. *Oncogene* **27,** 6434–51 (2008).

43. Matarrese, P. *et al.* Cathepsin B inhibition interferes with metastatic potential of human melanoma: an in vitro and in vivo study. *Mol. Cancer* **9,** 207 (2010).

44. Aits, S. & Jäättelä, M. Lysosomal cell death at a glance. *J. Cell Sci.* **126,** 1905–12 (2013).

45. Matte, I., Lane, D., Boivin, M., Rancourt, C. & Piché, A. MUC16 mucin (CA125) attenuates TRAIL-induced apoptosis by decreasing TRAIL receptor R2 expression and increasing c-FLIP expression. *BMC Cancer* **14,** 234 (2014).

46. Malhi, H., Guicciardi, M. E. & Gores, G. J. Hepatocyte Death: A Clear and Present Danger. *Physiol. Rev.* **90,** 1165–1194 (2010).

47. Conus, S. *et al.* Caspase-8 is activated by cathepsin D initiating neutrophil apoptosis during the resolution of inflammation. *J. Exp. Med.* **205,** 685–698 (2008).

48. Masson, O. *et al.* Pathophysiological functions of cathepsin D: Targeting its catalytic activity versus its protein binding activity? *Biochimie* **92,** 1635–43 (2010).

49. Minarowska, A., Minarowski, L., Karwowska, A. & Gacko, M. Regulatory role of cathepsin D in apoptosis. *Folia Histochem. Cytobiol.* **45,** 159–63 (2007).

50. Racusen, L. C. *et al.* Cell lines with extended in vitro growth potential from human renal proximal tubule: characterization, response to inducers, and comparison with established cell lines. *J. Lab. Clin. Med.* **129,** 318–29 (1997).

51. Rampersad, S. N. Multiple Applications of Alamar Blue as an Indicator of Metabolic Function and Cellular Health in Cell Viability Bioassays. *Sensors* **12,** 12347–12360 (2012).

52. Sorrells, S., Toruno, C., Stewart, R. A. & Jette, C. Analysis of Apoptosis in Zebrafish Embryos by Whole-mount Immunofluorescence to Detect Activated Caspase 3. *J. Vis. Exp.* (2013). doi:10.3791/51060

53. Ahmed, S. A. & Hamed, M. A. Kidney injury molecule-1 as a predicting factor for inflamed kidney, diabetic and diabetic nephropathy Egyptian patients. *J. Diabetes Metab. Disord.* **14,** 6 (2015).

54. Johansson, A.-C. *et al.* Regulation of apoptosis-associated lysosomal membrane permeabilization. *Apoptosis* **15,** 527–540 (2010).

55. Onishi, R. M. & Gaffen, S. L. Interleukin-17 and its target genes: mechanisms of interleukin-17 function in disease. *Immunology* **129,** 311–321 (2010).

56. Havasi, A. & Borkan, S. C. Apoptosis and acute kidney injury. *Kidney Int.* **80,** 29–40 (2011).

57. Padanilam, B. J. Cell death induced by acute renal injury: a perspective on the contributions of apoptosis and necrosis. *Am. J. Physiol. Renal Physiol.* **284,** F608–27 (2003).

58. Conus, S. & Simon, H.-U. Cathepsins and their involvement in immune responses. *Swiss Med. Wkly.* **140,** w13042 (2010).

59. Siedlecki, A., Irish, W. & Brennan, D. C. Delayed Graft Function in the Kidney Transplant. *Am. J. Transplant.* **11,** 2279–2296 (2011).

60. Joung, K.-W. *et al.* Incidence and Risk Factors of Acute Kidney Injury after Radical Cystectomy: Importance of Preoperative Serum Uric Acid Level. *Int. J. Med. Sci.* **12,** 599–604 (2015).

61. Hotchkiss, R. S., Strasser, A., McDunn, J. E. & Swanson, P. E. Cell Death. *N. Engl. J. Med.* **361,** 1570–1583 (2009).

62. Droga-Mazovec, G. *et al.* Cysteine cathepsins trigger caspase-dependent cell death through cleavage of bid and antiapoptotic Bcl-2 homologues. *J. Biol. Chem.* **283,** 19140–50 (2008).

63. Los, M. *et al.* Activation and caspase-mediated inhibition of PARP: a molecular switch between fibroblast necrosis and apoptosis in death receptor signaling. *Mol. Biol. Cell* **13,** 978–88 (2002).

64. Goto, M., Mizunashi, K., Kimura, N. & Furukawa, Y. Decreased sensitivity of distal nephron and collecting duct to parathyroid hormone in pseudohypoparathyroidism type I. *J. Am. Soc. Nephrol.* **12,** 1965–70 (2001).

65. Bennett, M. *et al.* Urine NGAL Predicts Severity of Acute Kidney Injury After Cardiac Surgery: A Prospective Study. *Clin. J. Am. Soc. Nephrol.* **3,** 665–673 (2008).

66. de Mendonça, A. *et al.* Acute renal failure in the ICU: risk factors and outcome evaluated by the SOFA score. *Intensive Care Med.* **26,** 915–21 (2000).

67. Coca, S. G., Yusuf, B., Shlipak, M. G., Garg, A. X. & Parikh, C. R. Long-term risk of mortality and other adverse outcomes after acute kidney injury: a systematic review and meta-analysis. *Am. J. Kidney Dis.* **53,** 961–73 (2009).

68. Haase, M., Haase-Fielitz, A., Bagshaw, S. M., Ronco, C. & Bellomo, R. Cardiopulmonary bypass-associated acute kidney injury: a pigment nephropathy? *Contrib. Nephrol.* **156,** 340–53 (2007).

69. Mrkobrada, M. *et al.* Need for Quality Improvement in Renal Systematic Reviews. *Clin. J. Am. Soc. Nephrol.* **3,** 1102–1114 (2008).

70. Hengartner, M. O. The biochemistry of apoptosis. *Nature* **407,** 770–6 (2000).

71. Turk, B. *et al.* Apoptotic pathways: involvement of lysosomal proteases. *Biol. Chem.* **383,** 1035–44

72. Turk, B. & Stoka, V. Protease signalling in cell death: caspases versus cysteine cathepsins. *FEBS Lett.* **581,** 2761–7 (2007).

73. Sakai, H., Saku, T., Kato, Y. & Yamamoto, K. Quantitation and immunohistochemical localization of cathepsins E and D in rat tissues and blood cells. *Biochim. Biophys. Acta* **991,** 367–75 (1989).

74. Aregger, F. *et al.* Identification of IGFBP-7 by urinary proteomics as a novel prognostic marker in early acute kidney injury. *Kidney Int.* **85,** 909–19 (2014).

75. Roberg, K., Kågedal, K. & Öllinger, K. Microinjection of Cathepsin D Induces Caspase-Dependent Apoptosis in Fibroblasts. *Am. J. Pathol.* **161,** 89–96 (2002).

76. Lagadic-Gossmann, D., Huc, L. & Lecureur, V. Alterations of intracellular pH homeostasis in apoptosis: origins and roles. *Cell Death Differ.* **11,** 953–61 (2004).

77. Li, X., Koh, Y. & Engelman, A. Correlation of Recombinant Integrase Activity and Functional Preintegration Complex Formation during Acute Infection by Replication-Defective Integrase Mutant Human Immunodeficiency Virus. *J. Virol.* **86,** 3861–3879 (2012).

78. Gacko, M., Minarowska, A., Karwowska, A. & Minarowski, Ł. Cathepsin D inhibitors. *Folia Histochem. Cytobiol.* **45,** 291–313 (2007).

79. Koike, M. *et al.* Participation of autophagy in storage of lysosomes in neurons from mouse models of neuronal ceroid-lipofuscinoses (Batten disease). *Am. J. Pathol.* **167,** 1713–28 (2005).

80. Steinfeld, R. *et al.* Cathepsin D deficiency is associated with a human neurodegenerative disorder. *Am. J. Hum. Genet.* **78,** 988–98 (2006).

81. Siintola, E. *et al.* Cathepsin D deficiency underlies congenital human neuronal ceroid-lipofuscinosis. *Brain* **129,** 1438–45 (2006).

82. Gross, F., Lazar, J. & Orth, H. Inhibition of the renin-angiotensinogen reaction by pepstatin. *Science* **175,** 656 (1972).

83. Conus, S. *et al.* Caspase-8 is activated by cathepsin D initiating neutrophil apoptosis during the resolution of inflammation. *J. Exp. Med.* **205,** 685–98 (2008).

84. Roberg, K., Johansson, U. & Ollinger, K. Lysosomal release of cathepsin D precedes relocation of cytochrome c and loss of mitochondrial transmembrane potential during apoptosis induced by oxidative stress. *Free Radic. Biol. Med.* **27,** 1228–37 (1999).

85. Chipuk, J. E., Moldoveanu, T., Llambi, F., Parsons, M. J. & Green, D. R. The BCL-2 family reunion. *Mol. Cell* **37,** 299–310 (2010).

86. Appelqvist, H. *et al.* Lysosome-mediated apoptosis is associated with cathepsin D-specific processing of bid at Phe24, Trp48, and Phe183. *Ann.*

Clin. Lab. Sci. **42,** 231–42 (2012).

87. Fox, C. *et al.* Inhibition of lysosomal protease cathepsin D reduces renal fibrosis in murine chronic kidney disease. *Sci. Rep.* **6,** 20101 (2016).

88. Mejia, A. & Kraft, W. K. Acid peptic diseases: pharmacological approach to treatment. *Expert Rev. Clin. Pharmacol.* **2,** 295–314 (2009).